New results from the sensor human brain project alternative

Ruedi Stoop,
Albert Kern, Jan-Jan van der Vyver,
Stefan Martignoli, Florian Gomez,
Tom Lorimer, Karlis Kanders,
Karolina Ignatiadis

Institute of Neuroinformatics UNI / ETH of Zurich

Focus of the century: Understanding the brain

- **Human brain project:**
  Aims at accomplishing the goal by re-building the brain physiology (reminds me of Chomsky's critique regarding understanding the nature of language!)

Old results that made us look for an alternative approach…

Starting 1996 @ ini UZH/ETHZ: Experiments on rat somatosensory neurons

'NEURONS ARE (JUST) OSCILLATORS' (E. Moses, Madrid 2018)

Experiments (1996/7, K. Schindler, L. Bunimovich)

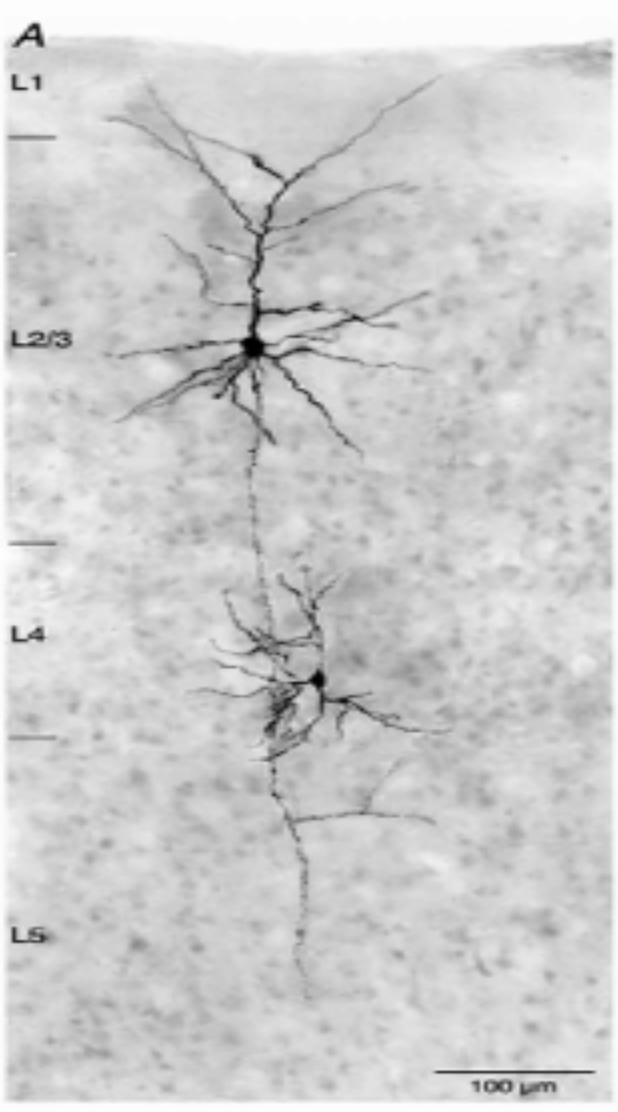

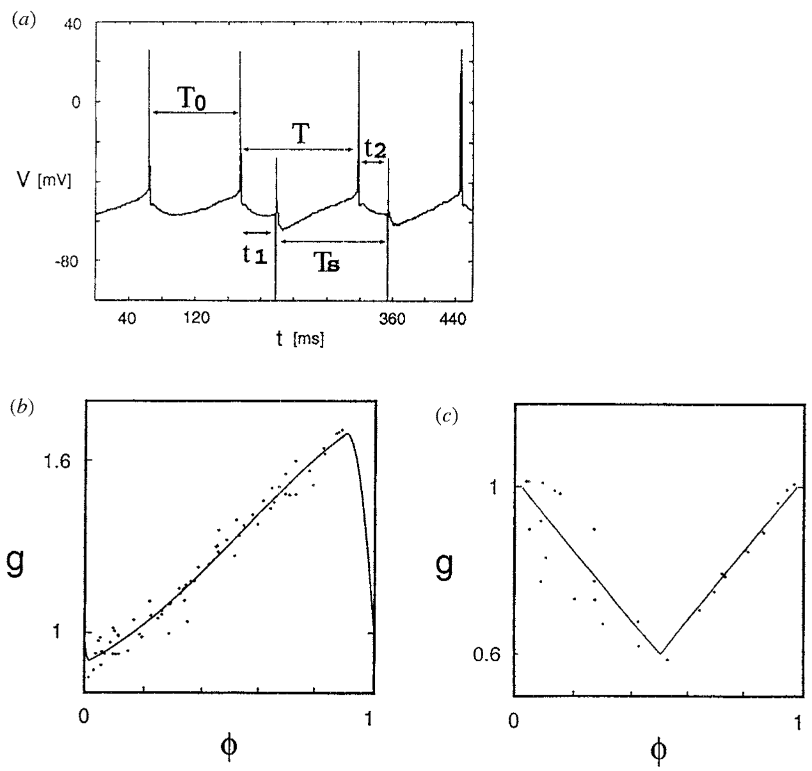

$$\phi_2 = \phi_1 + \Omega - g(\phi_1) \quad \mathrm{mod}(1)$$

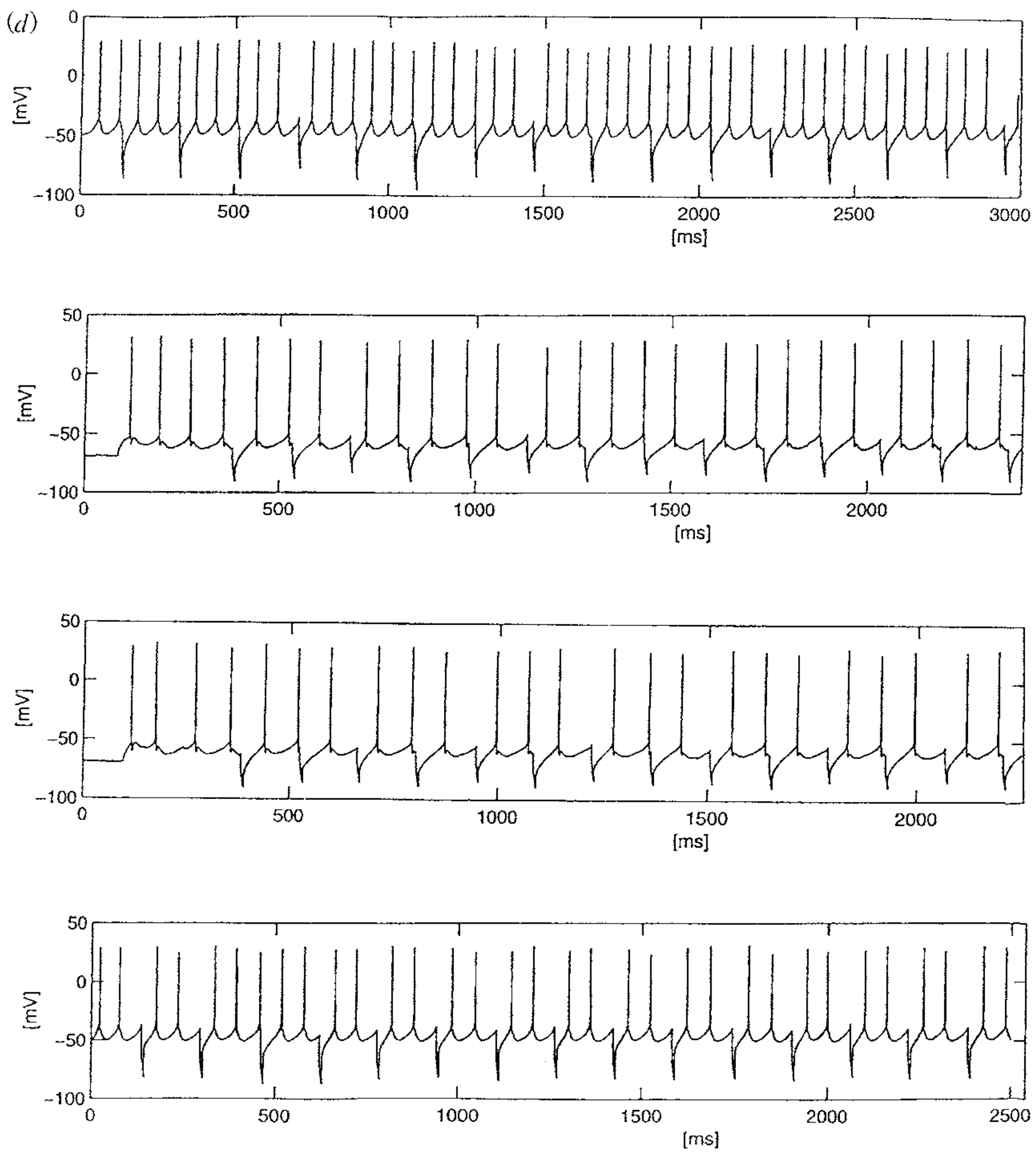

Numerical explorations:

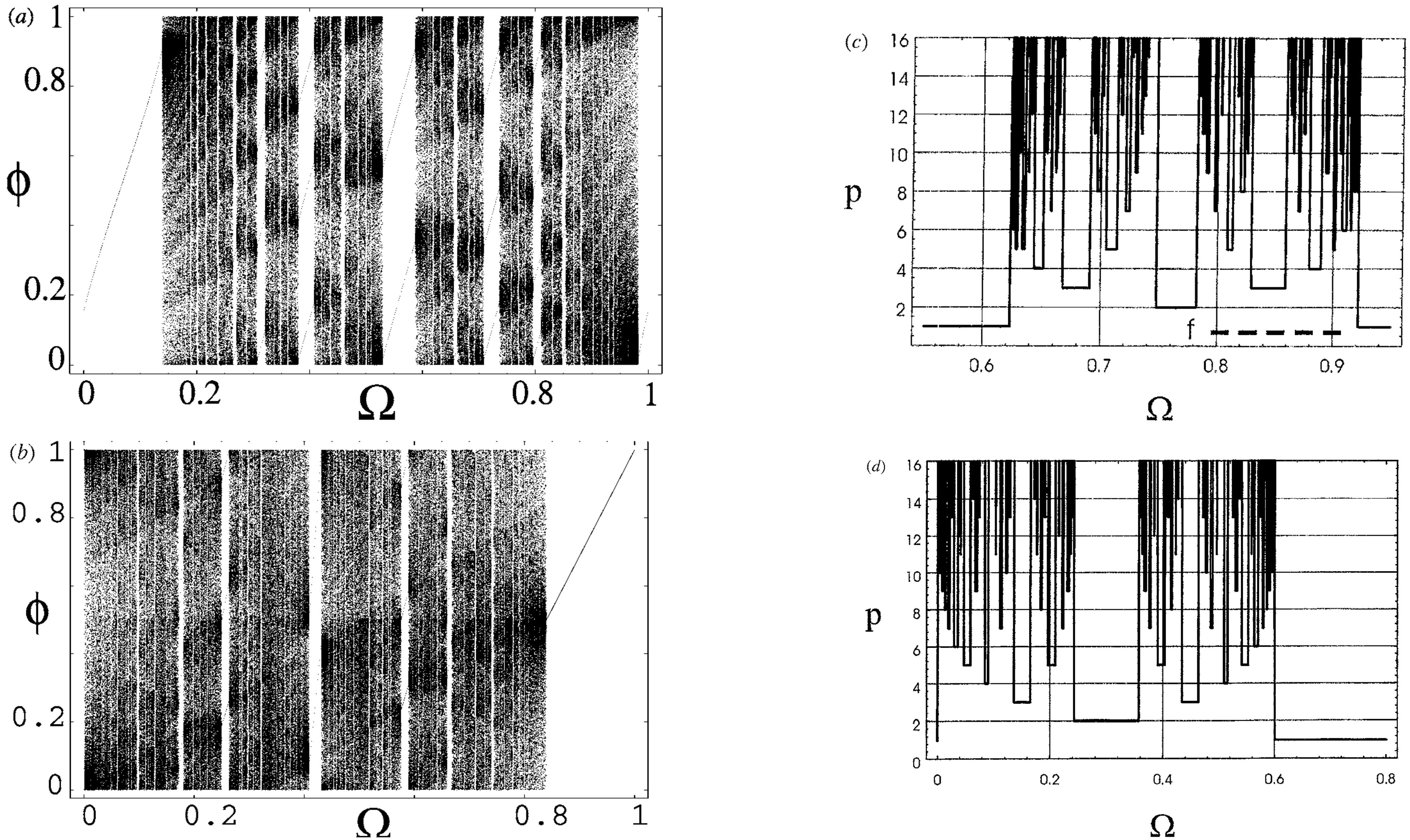

Comparison experiment-simulation:

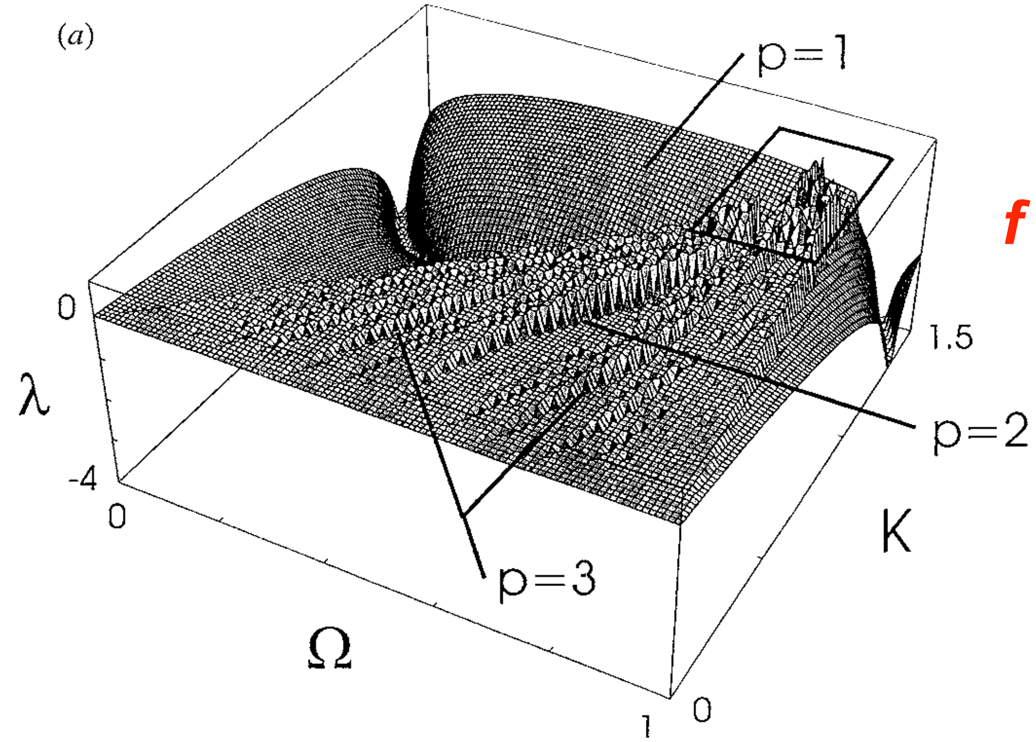

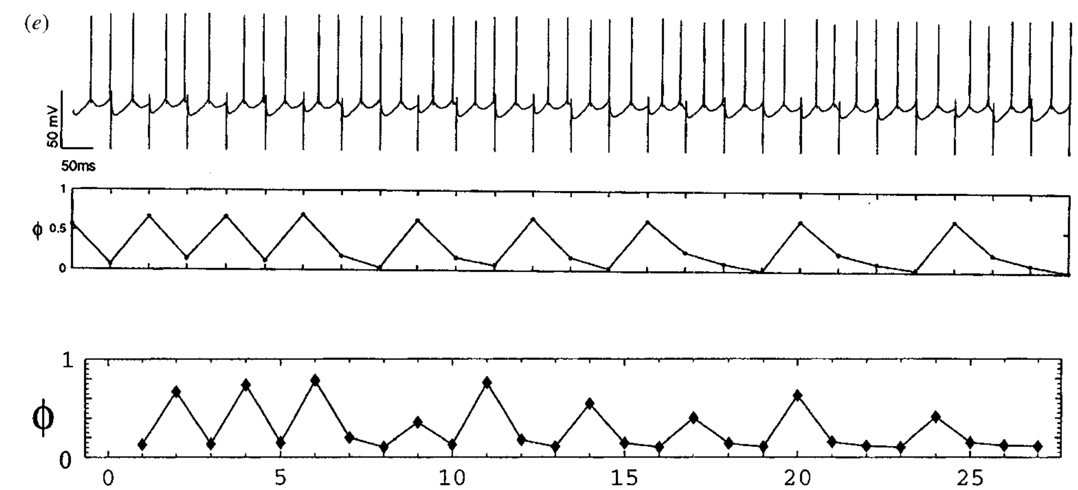

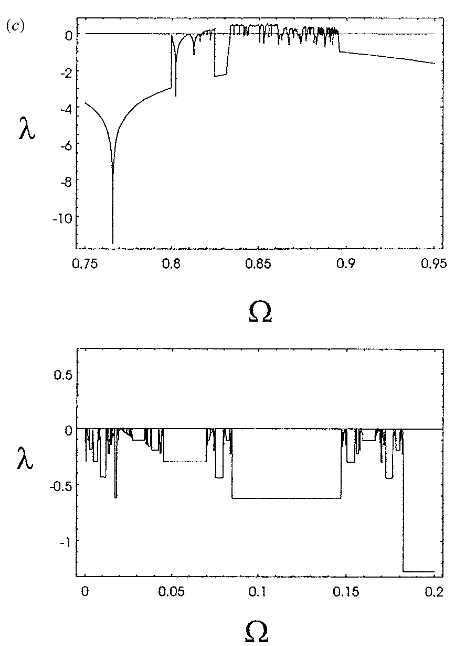

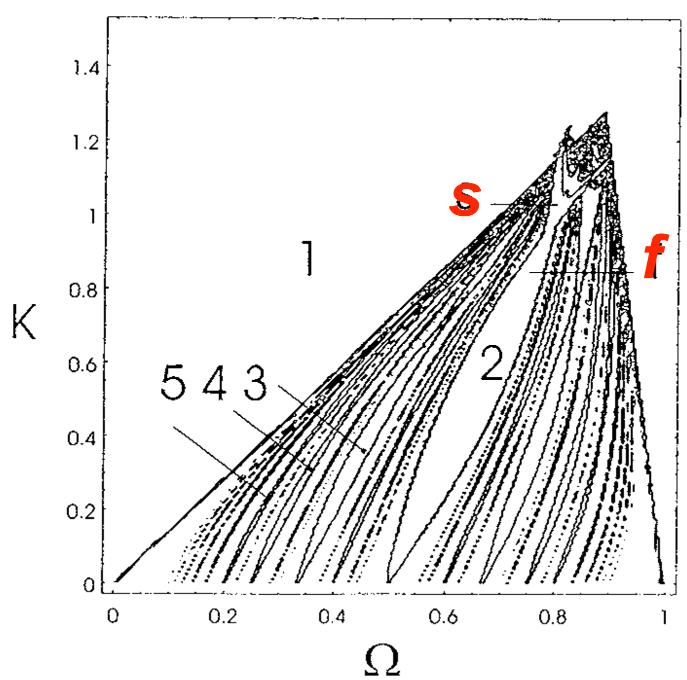

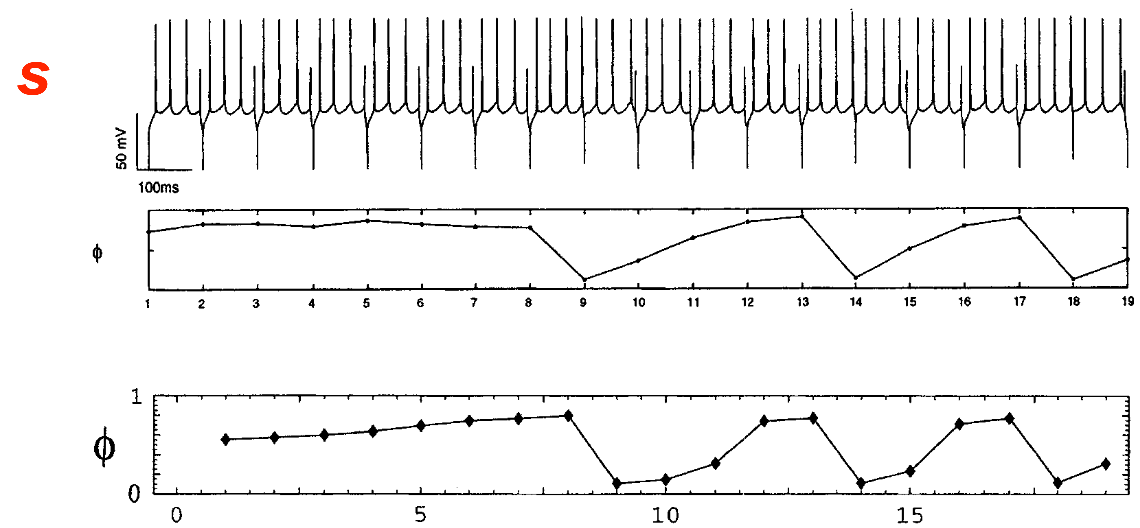

More recent generalizations:
S. Martignoli
K. Kanders

Interacting neuron pairs (1998):

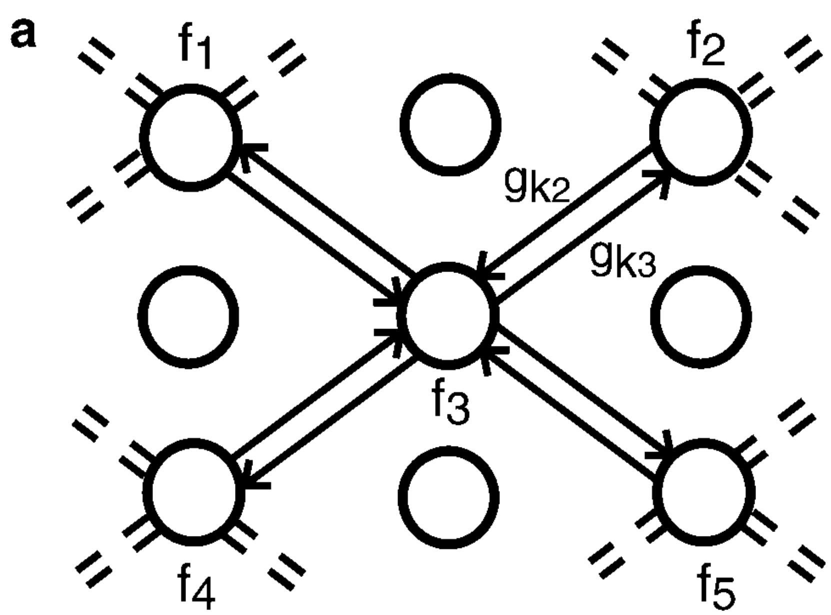

$$\phi\{i,j\}(t_{n+1}) := (1 - k_2 k\{i,j\}) f_{K\Omega}(\phi\{i,j\}(t_n)) + k_2/nn\ k\{i,j\} \sum_{nn} \phi\{k,l\}(t_n)$$

1-d chain of diffusively coupled (binary) interaction maps:

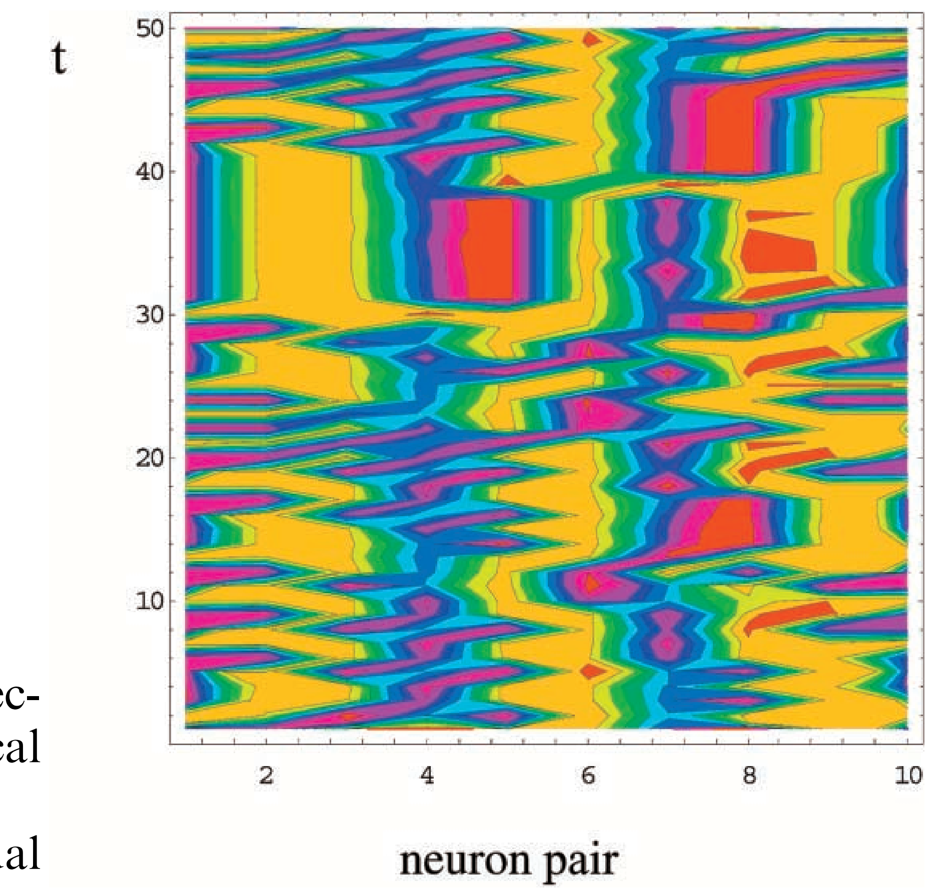

Stoop R, Schindler K, Bunimovich LA (1999) Inhibitory connections enhance pattern recurrence in networks of neocortical pyramidal cells. Phys Lett A 258: 115–122

Stoop R, Schindler K, Bunimovich LA (2000a) When pyramidal neurons lock, when they respond chaotically, and when they like to synchronize. Neurosci Res 36: 81–91

Stoop R, Schindler K, Bunimovich LA (2000b) Noise-driven neocortical interaction: complex neuron spiking uncovered by nonlinear dynamics. Acta Biotheor 48: 149–171

Interacting neuron pairs (1998, RS,LAB, WHS):

1-d chain of diffusively coupled (binary) tent-map (slope a) interaction maps:

Phase-coincidence learning $k\{i,j\}(t_{n+1}) := k\{i,j\}(t_n)(\mathrm{Tanh}[r]+1)/2$

(binary) tent-map (slope a) interaction maps

(r=sum of absolute inverse phase differences)

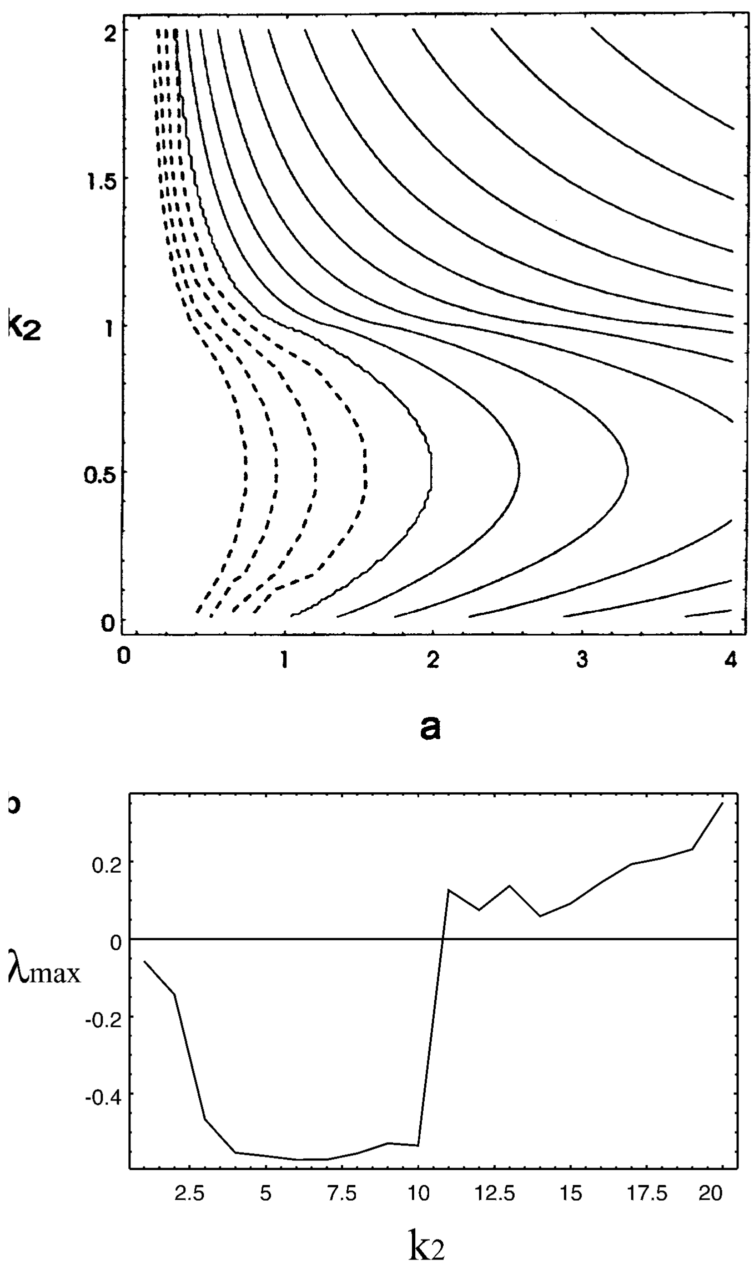

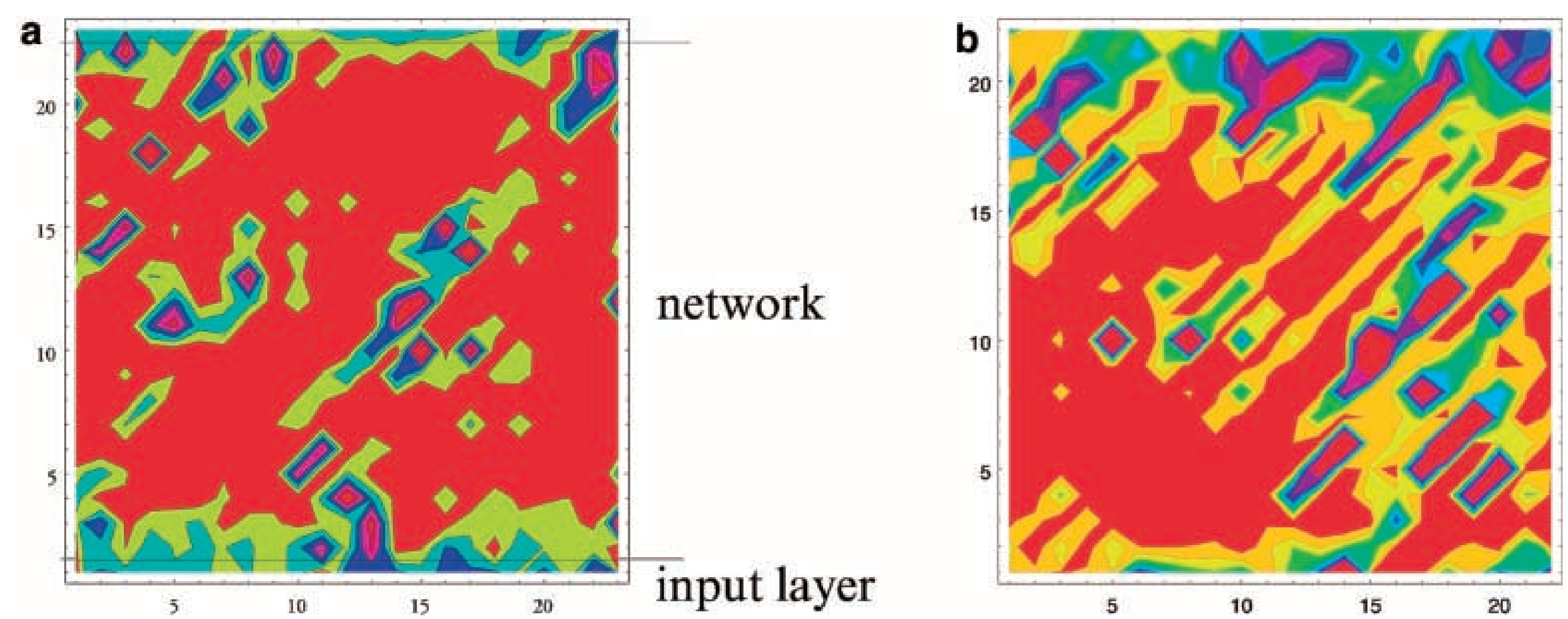

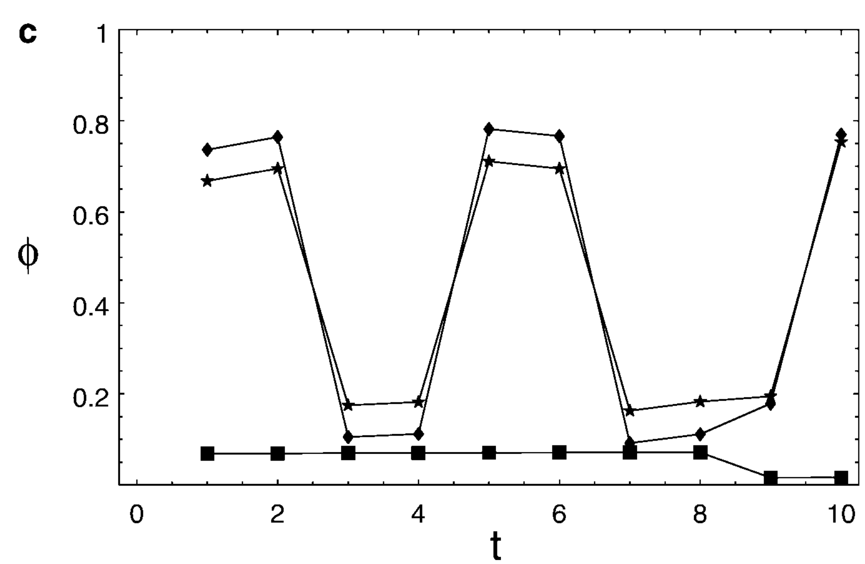

Fig. 8. **a** Phase differences evoked by two distinct input patterns (2-d network, evolution under phase-coincidence detection). In the *red area*, no changes are observed. The *bottom layer* (= input layer) shows the differences in the input patterns. Due to two-torus periodic boundary conditions, this also affects the top layer. Coding sites are the islands within the red sea. At these sites, prominent phase changes are observed. **b** Corresponding figure when excitatory phase return maps have extended refractory periods. A visibly increased "penetration depth" of coding sites indicates increased degree of synchronization. **c** Temporal phase difference evolution, at a coding site from (**a**). Three input signals were compared (constant random phase layer l_1, constant layer l_2 with phase 0.2, constant layer l_3 with phase 0.6). Absolute phase differences are shown of, *top curve*: $l_1 - l_2$, *medium curve*: $l_1 - l_3$, *bottom curve*: $l_2 - l_3$

Next level: What's in cortical columns?

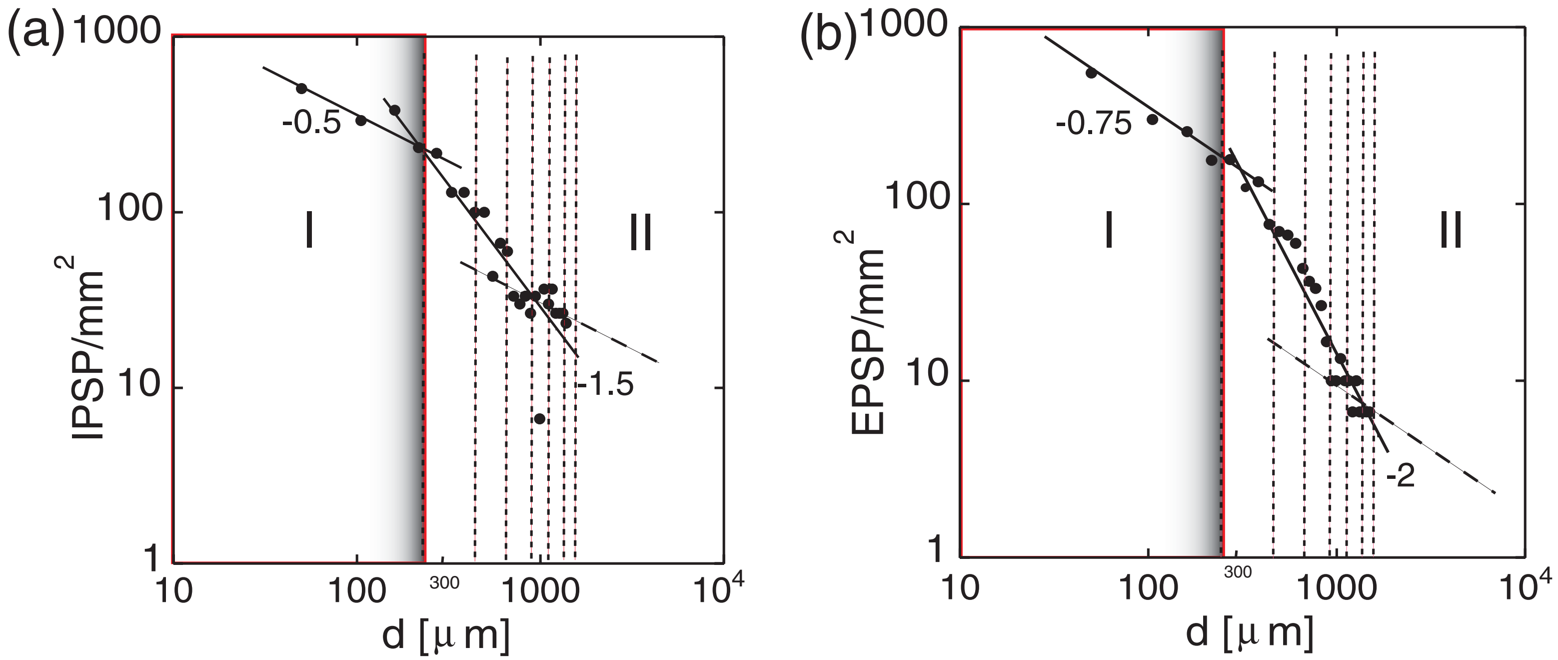

double power-law!

Log-density of photostimulation—evoked excitatory (a) and inhibitory (b) synaptic inputs (concentric rings 50 μm apart, from 19 pooled layer 2/3 neurons). (I): Inner-columnar, (II): Intercolumnar scale. Vertical lines: Extensions of aligned physiological columns. Tilted dashed lines: Proposed long distance decay.

B. Roerig and B. Chen, Cereb. Cortex **12**, 187 (2002).

Testing the ‘canonical microcircuit’ dogma

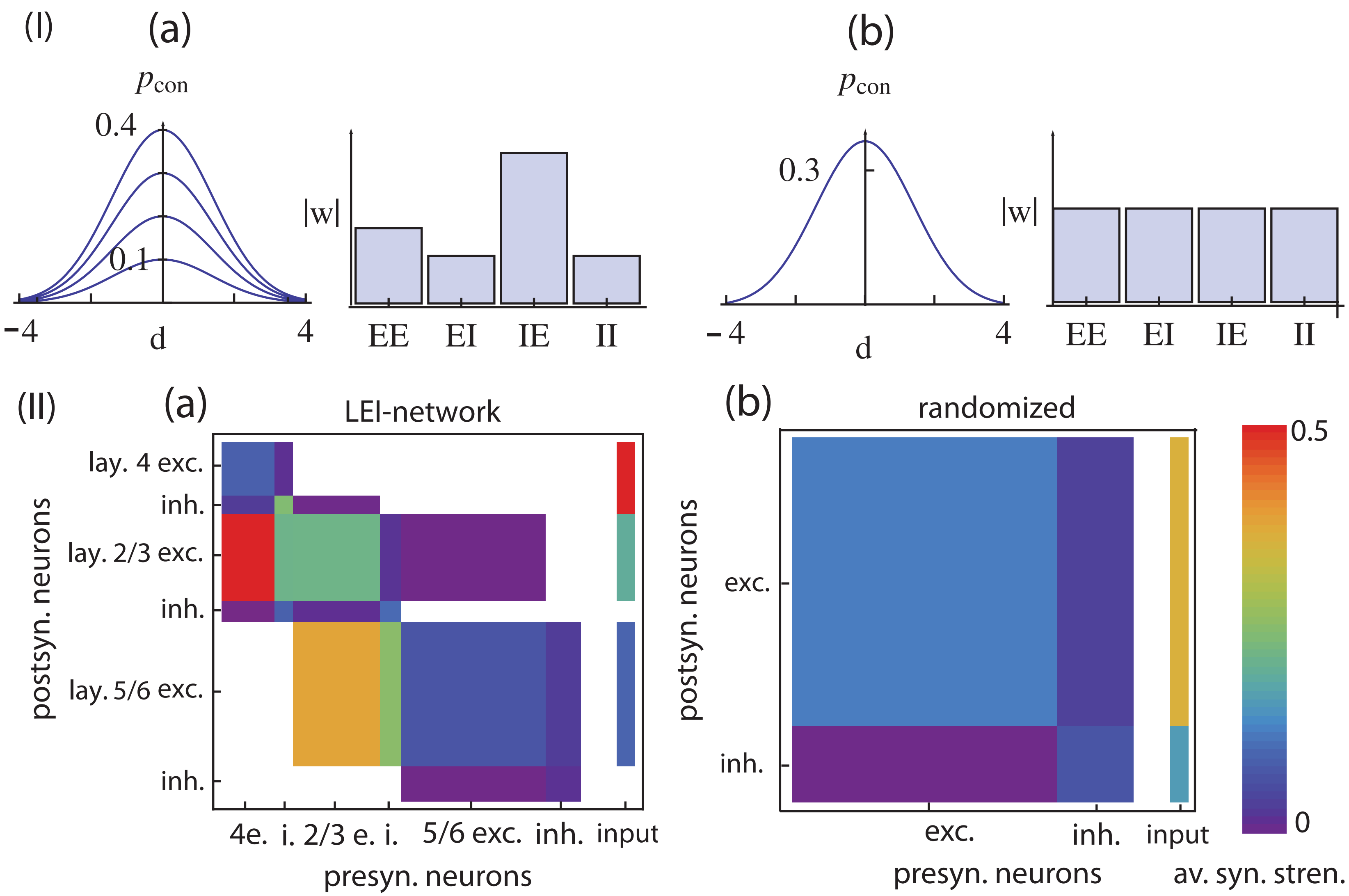

(I) (a) EI model, (b) EI-control network (uniform synaptic weights w, $\lambda = 2$). p_{con}: probability of a synaptic connection among neurons of distance d for C values as in the text, w: synaptic strength of the connections. (II) (a) LEI-model, (b) LEI-control network. Input strengths to populations are color coded.

‘reservoir computing’

Columnar wiring does not matter, except for..

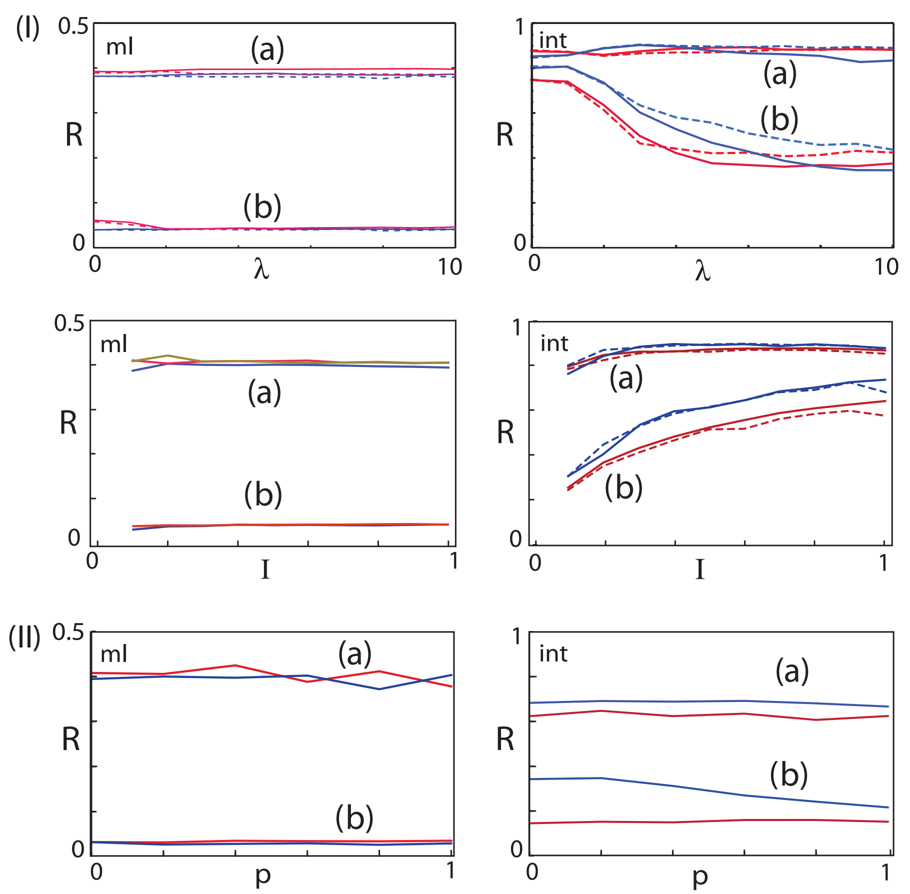

Recognition rate R for (a) Arabic Digit, and (b) Auslan recognition. Each data point represents an average over at least 20 experiments following a normal-like distribution each [cf. Supplemental Material Sec. (1b) [10]]. Blue: leaky integrate and fire, red: Izhikevich neurons. Left column: memoryless (ml), right column: integration (int) readout. (I) *EI* network, dependence on rewiring parameter λ (control networks: dashed curves), and on ratio I of input receiving neurons, at local connectivity (i.e., $\lambda = 2$). Ocher: Izhikevich neurons with $\lambda = 0$. (II) *LEI* networks, dependence on rewiring probability p. $p = 0$: layered, $p = 1$: homogeneous control network.

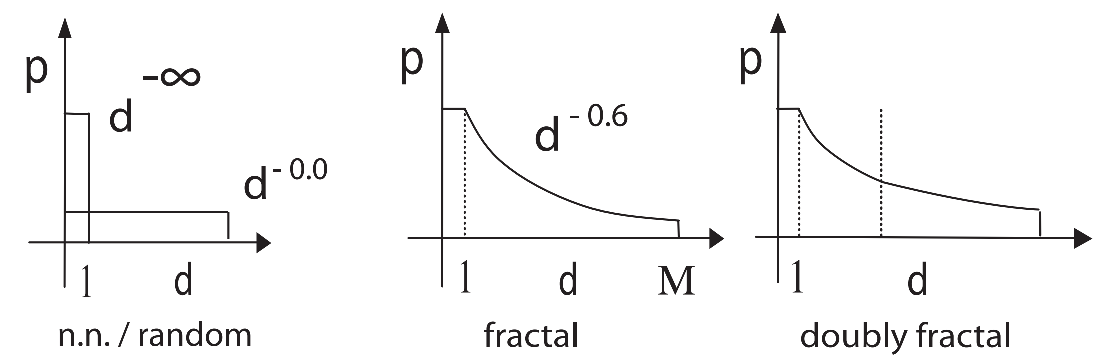

Main connectivity classes compared (p: connection probabilities, d: distance, M: cutoff, see text).

double power-law connectivty matters

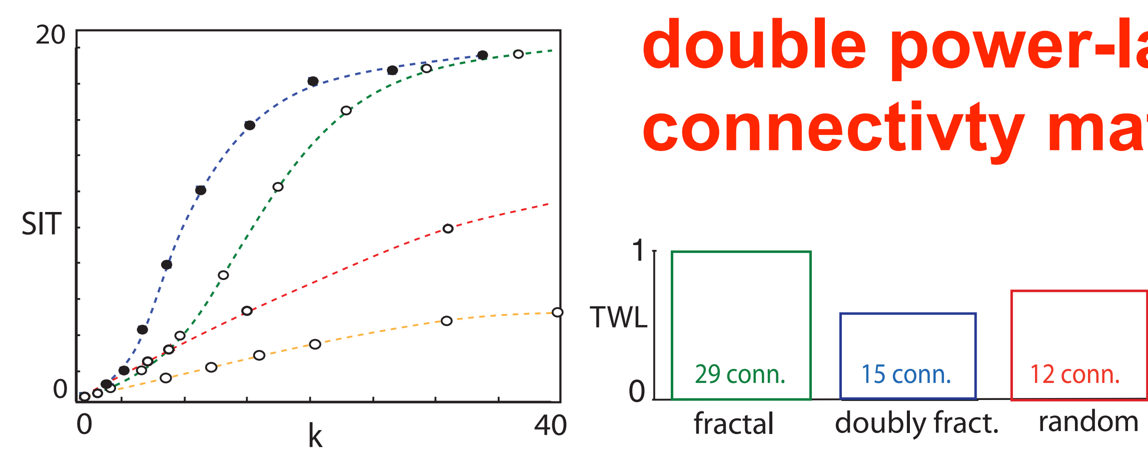

Left: SIT as a function of cell connections k. From top: doubly fractal ($\theta = 0.2$, $\alpha = 0.5$, $\beta = 2.0$), fractal ($\theta = 1$, $\alpha = 0.7$), random, n.-n. topology. Network sizes: $N = 4096$, averages over 100 experiments. Right: Connections k_{min} required for synchronization, and associated TWL. $N = 512$, 10 experiments.

R.S et al PRL 2014

Follow the money… Change of approach: 'explain the brain'!

- > follow the information flow

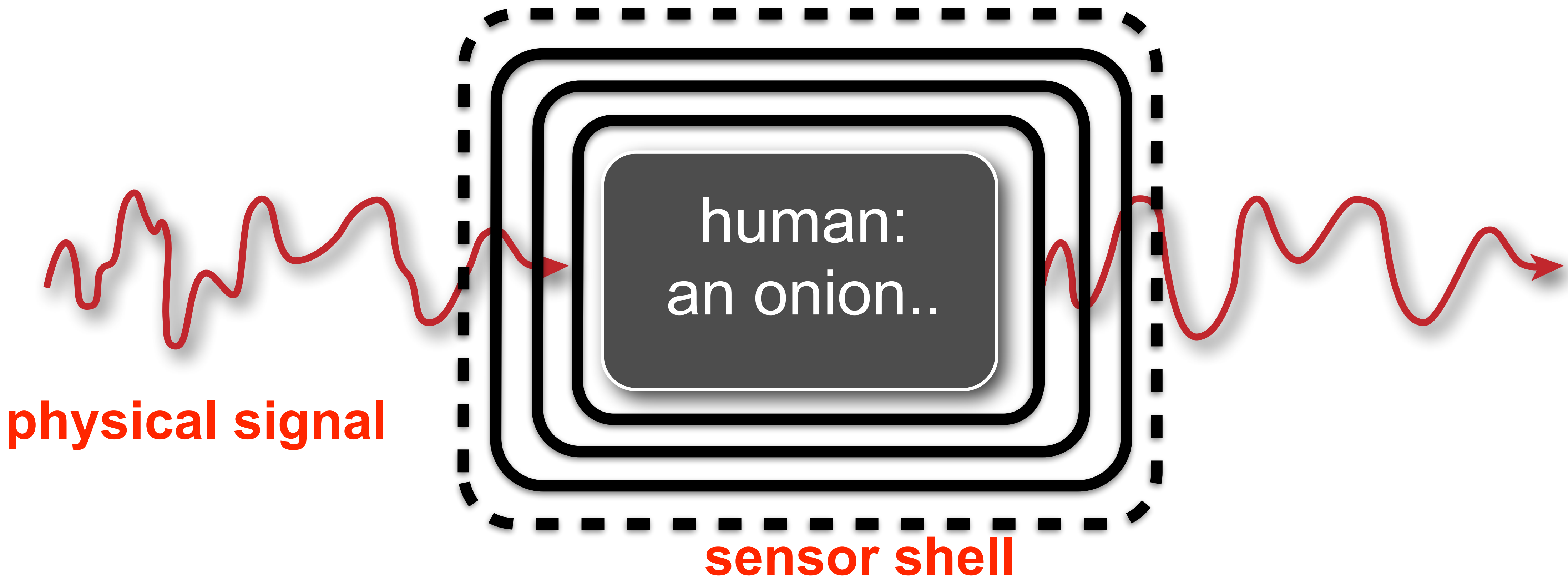

Hearing system properties:

- Ancestral to the nervous system
  (hope: explain aspects of the brain from the sensors' perspective)
- Verifiable ('big' unexplained data)
- Simple fundamental physics-based model
- Powerful if embedded into physiological context
- Explains a number of puzzling observations

Overview:

1995: Wiesenfeld: Small signal amplifiers, PRL
1999: Start: Kern-Stoop cochlea, from scratch, based on fluid dynamics, energy-based approach
2000: Eguiluz, PRL: Hopf concept
2002 Kern's thesis finished
2003: Kern & Stoop, PRL
2003: Comment to Magnasco's PRL
2004: Stoop & Kern, PRL, PNAS
2004: Efferent tuning, submitted to SNF
2005: Coupling reconsidered, v.d.Vyver
2005: Hardware cochlea, v.d.Vyver
2006: v.d.Vyver's thesis, ETHZ
2006: US Patent filed
2006: Insect hearing: Hopf in Drosophila antenna
2008: Cochlear re-mapping
2010: Local correlations of the perceived pitch, PRL
2011: Effect of Nuclei, NECO
2013: Pitch sensation involves stochastic resonance, Sci. Rep.
2014: Efferent tuning implements listening, Phys. Rev. Appl.
2014: Pitch sensation shaped by cochlear fluid, Nat. Phys.
2016: Signal-coupled subthreshold Hopf-type systems show sharpened collective response, PRL
2016: Auditory power-law activation avalanches exhibit a fundamental computational ground state, PRL
2017: Mammalian hearing threshold explained, Sci. Rep.
2018: "Harmony" perception explained from network principles

Q: What do we hear and why?

1840: Berlin vs. Dresden

Ohm

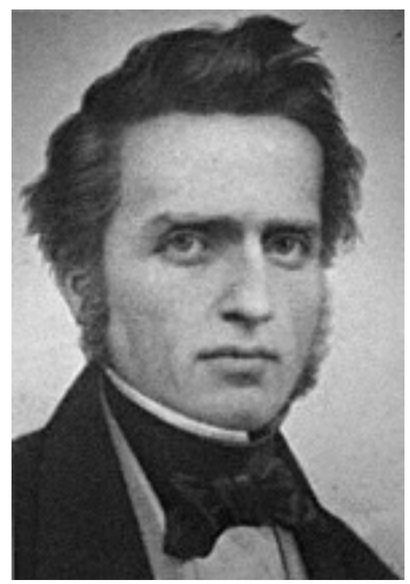

Seebeck

What is the physical description of ‘pitch’ sensation?

“Wodurch kann über die Frage, was zu einem Tone gehöre, entschieden werden, als eben durch das Ohr?”
(How else can the question as to what makes out a tone, be decided but by the ear?)

August Seebeck 1844

Mammalian cochlea

more than a frequency analyzer..

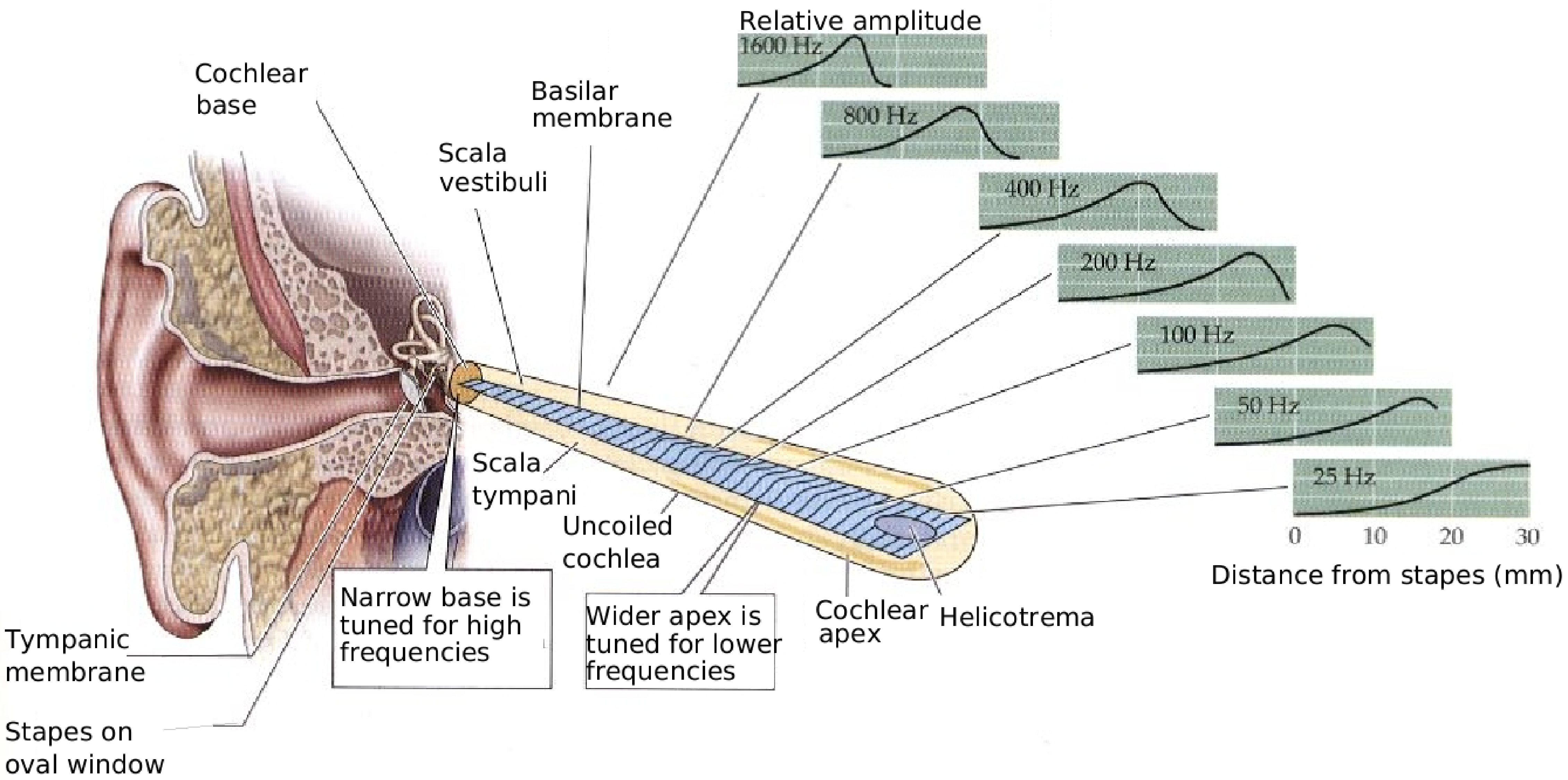

Experiments

- simple tone: A*sin(2*π*fo*t)

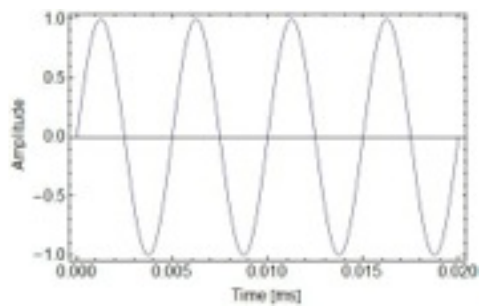

- complex tone:
(frequency components
fo, 2fo, 3fo, …)

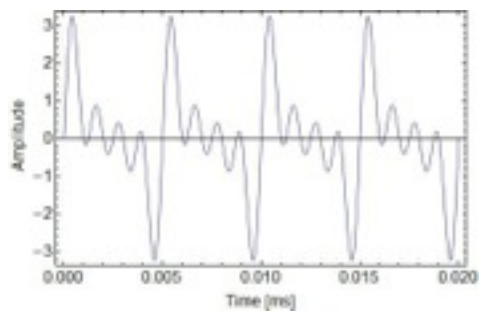

- missing fundamental

simple **complex** **missing fundamental**

- Smoorenburg's two-tone experiments:

1750/2000 ->1800/2000 Hz

reversed

pitch down (250 -> 200 Hz, fundamental), or pitch up ?

I Key for understanding hearing:
nonlinear ’small signal amplifier’

Wiesenfeld et al. PRL 1984/5/6:

Systems close to a **period-doubling bifurcation** can be used as a small signal amplifier:
Signals with a certain ‘critical’ frequency are strongly amplified.

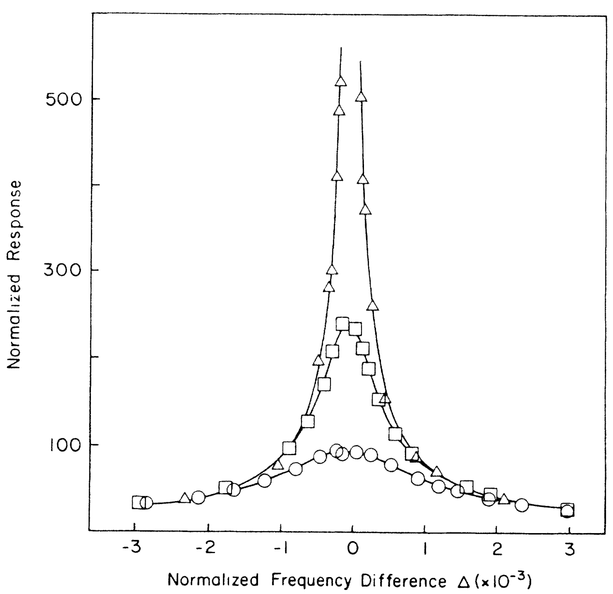

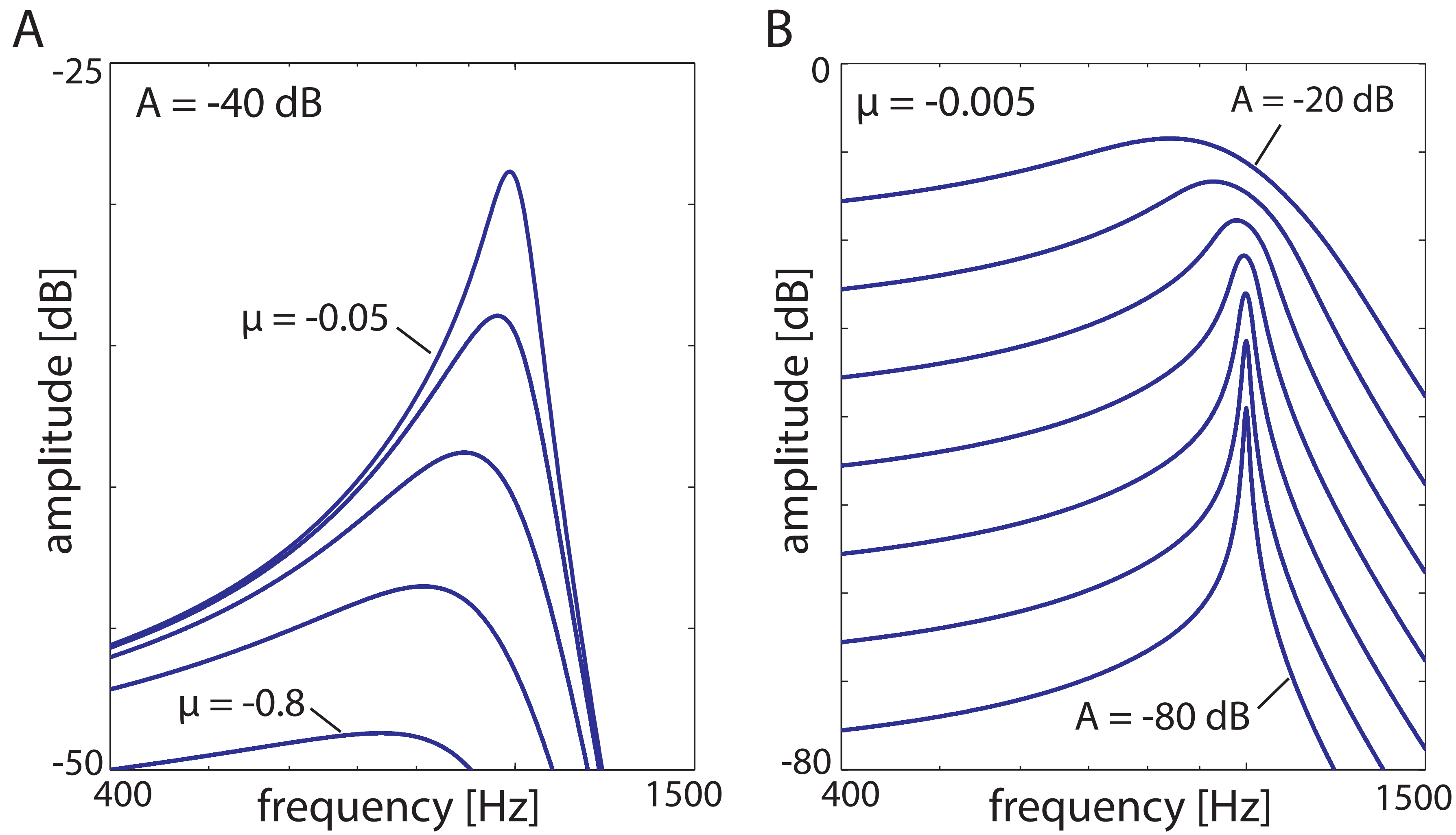

Andronov-Hopf: Brun at al., PRL 1985

Biological evidence of Hopf small signal amplifiers

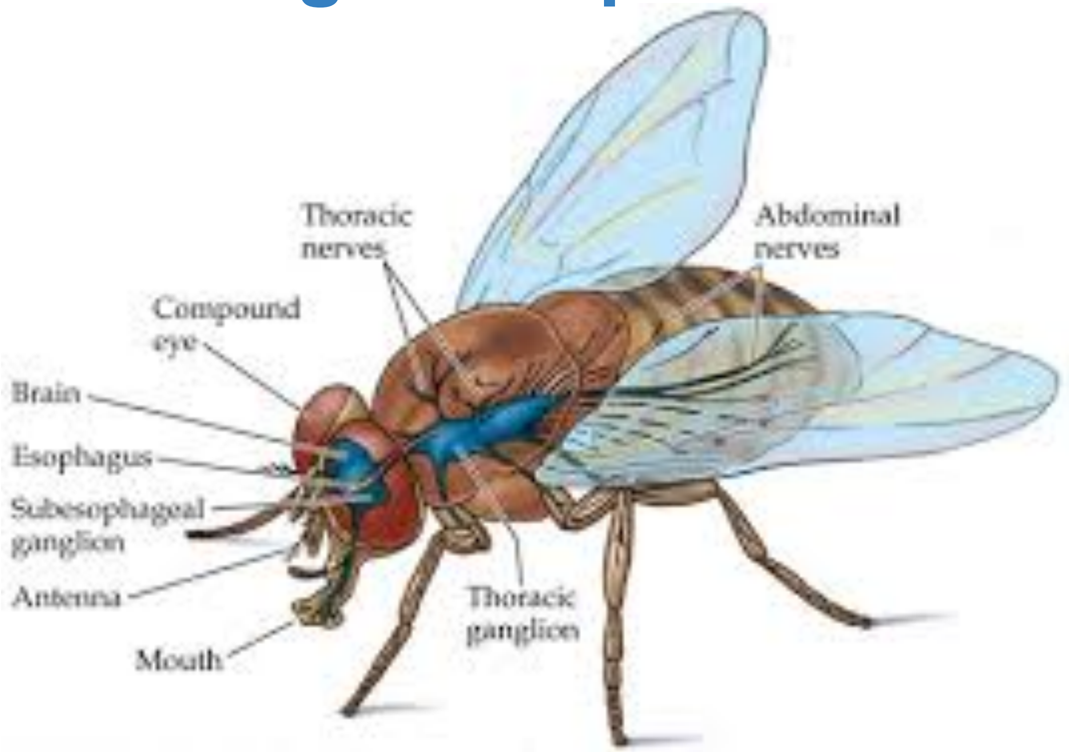

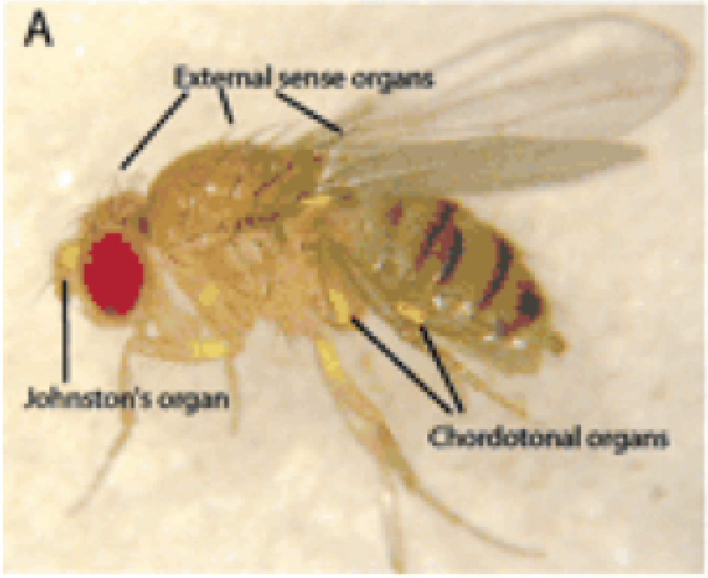

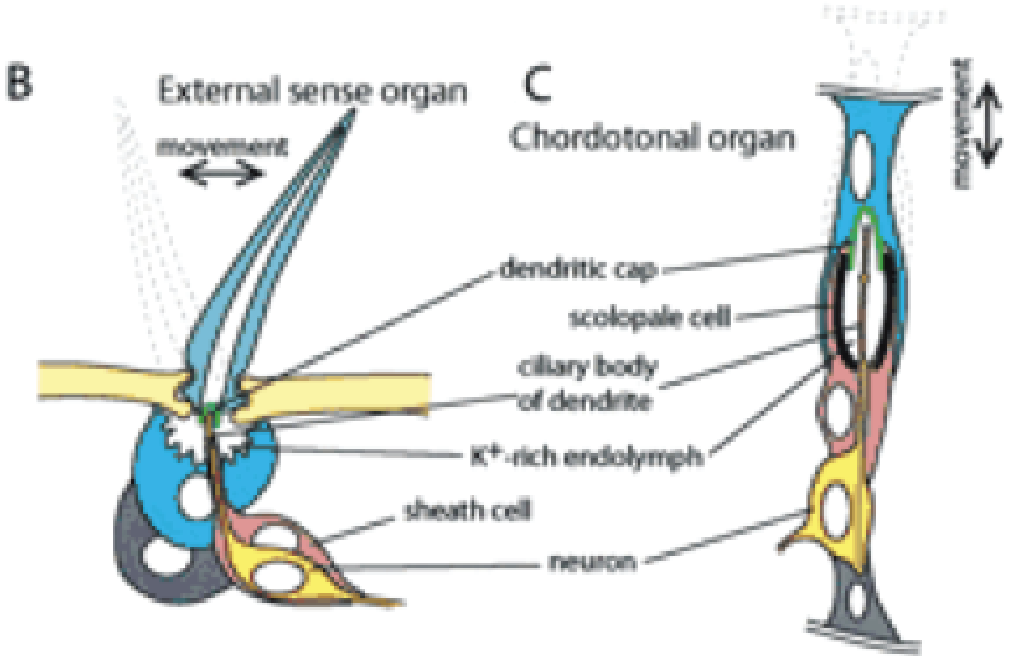

Dynamics above bifurcation demonstrate the Hopf property

$$\ddot{x} + P_n(x)\dot{x} + P_m(x) = 0$$
$$\ddot{x} - \mu(1 - x^2)\dot{x} + x = 0$$

Generalized van der Pol oscillator

$\mu=0$: A.-Hopf bifurcation

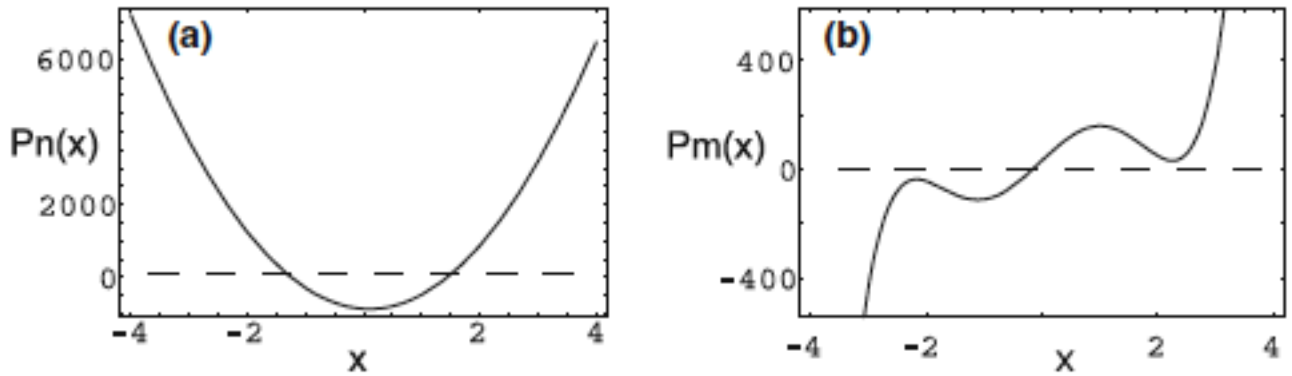

P’m(x), restoring force, negative stiffness

(P’m(x)<0: active amplification)

experiment

simulation

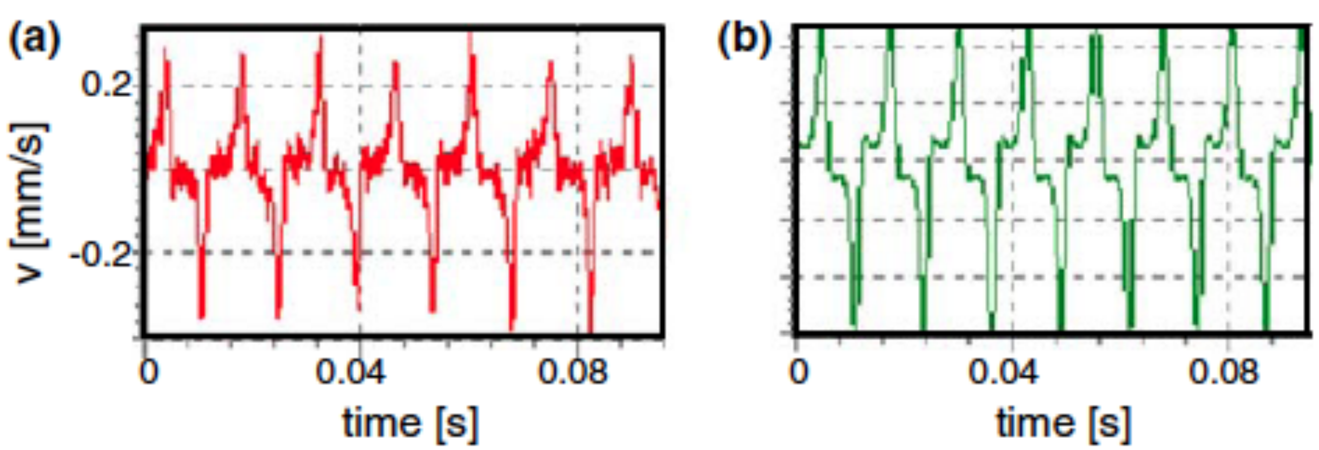

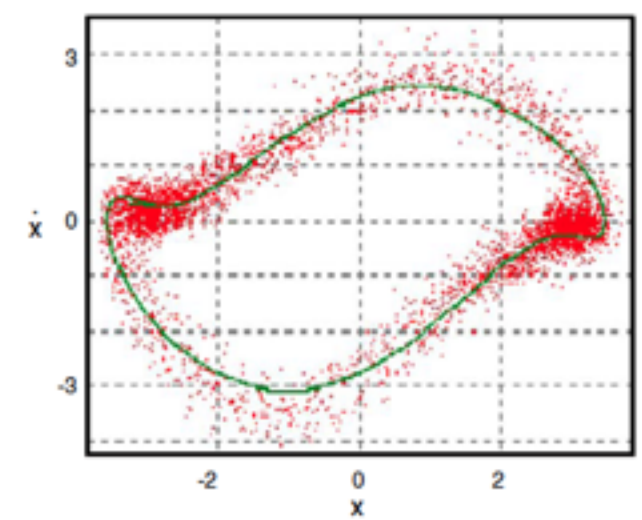

R.S. et al, Eur. Biophys. J. 2006
T.L., F.G. & R.S. Sci. Rep. 2015

Active response R from a forced Hopf system (F: forcing)

- Close to bifurcation point and resonance: $R = \boxed{F^{1/3}}$
- Before bifurcation point, small F: $R = -F/\mu$
- Charakteristic of Hopf-bifurcation

LogR

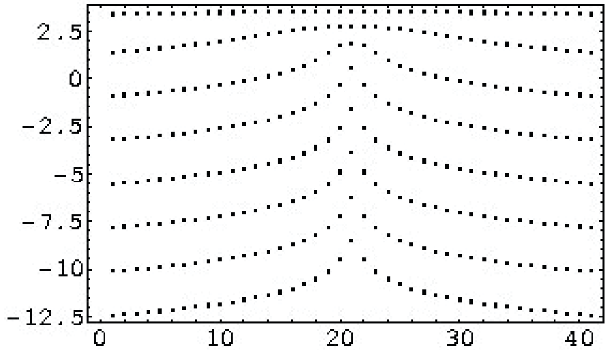

Frequency

wc =1000 Hz, μ = -20, governs G
F = {0.004 10^i, i=0..7}

(Eguiluz et al. PRL 2000)

II From many sensors to a cochlea:
the wiring problem

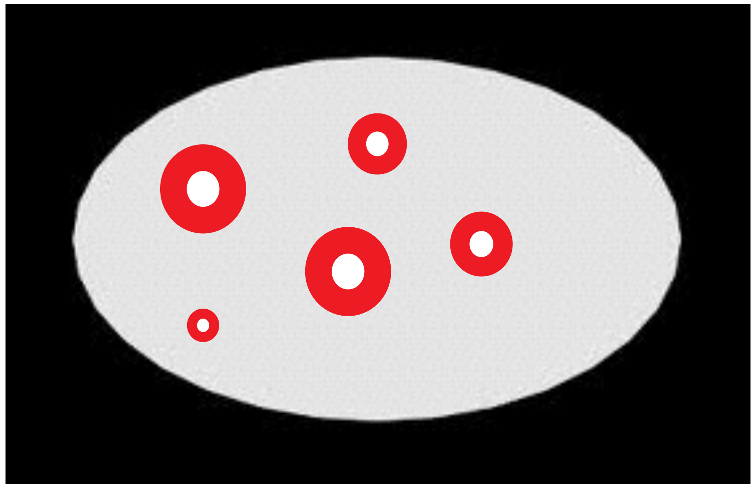

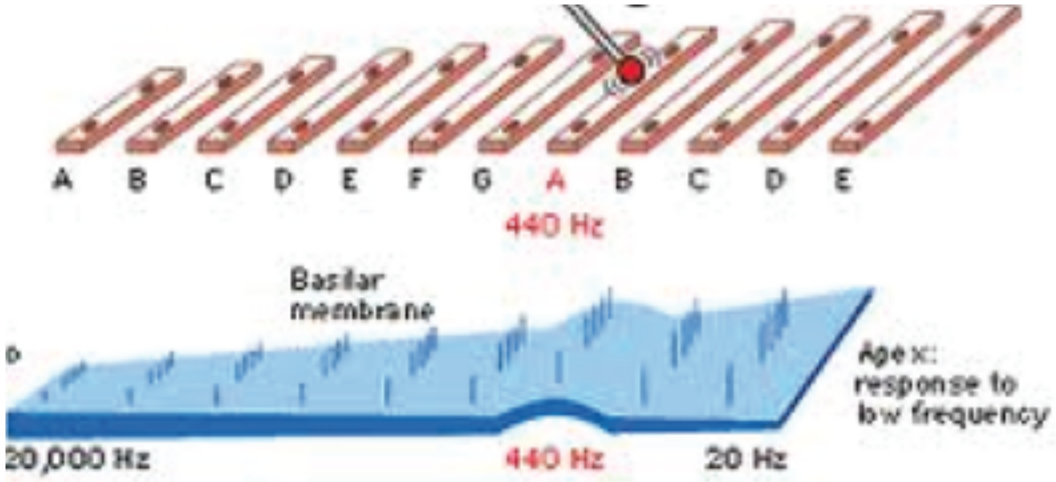

(Lorimer, Gomez, R.S., Sci. Rep. 2015)

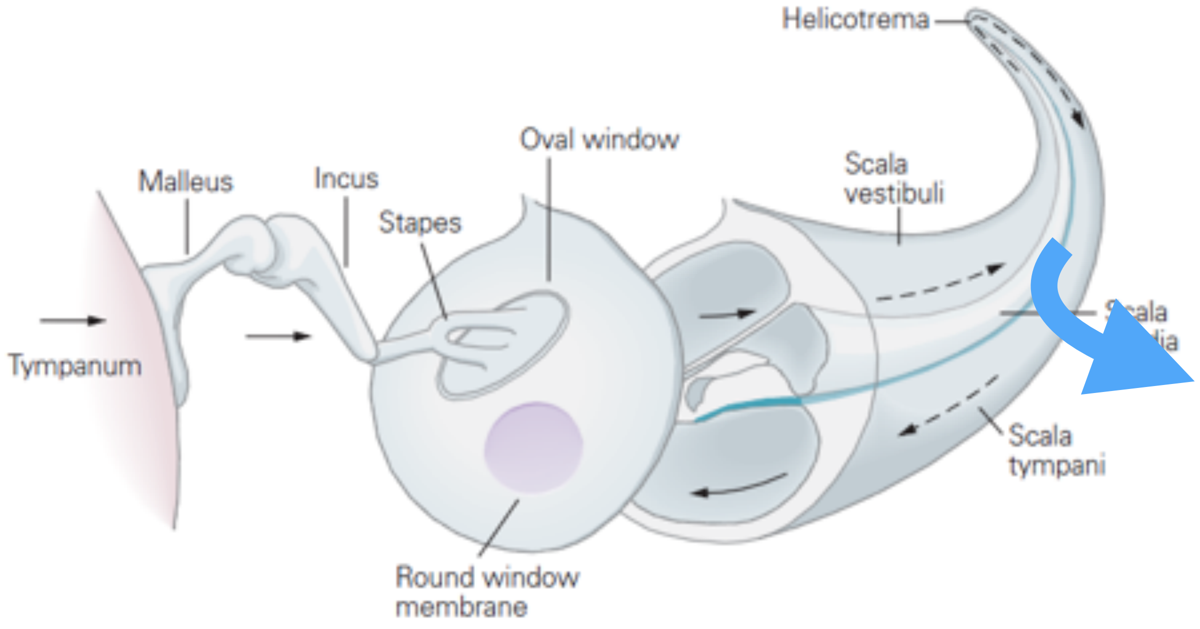

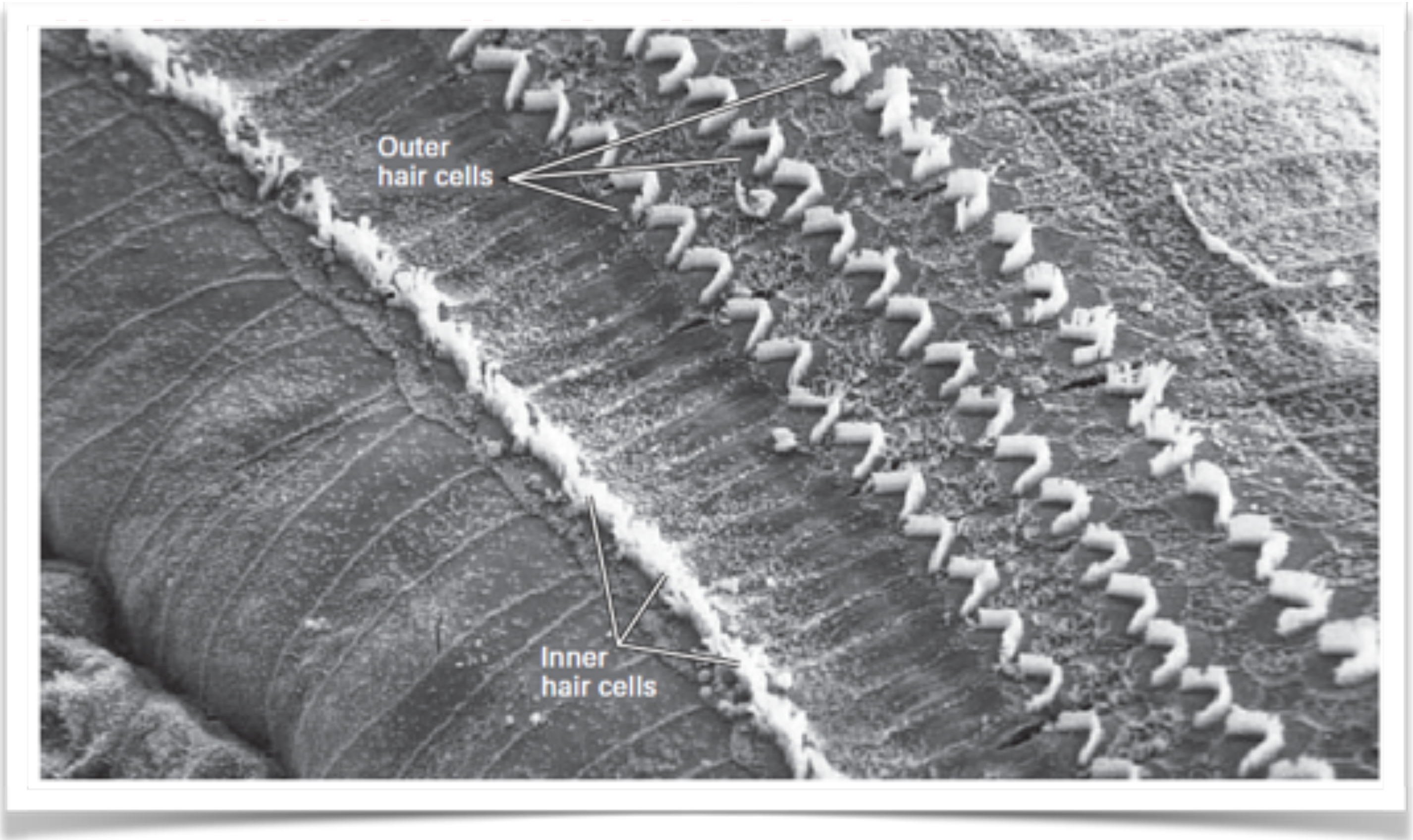

Hudspeth 2013

Generic properties:
Individual vs. signal-coupled Hopf elements

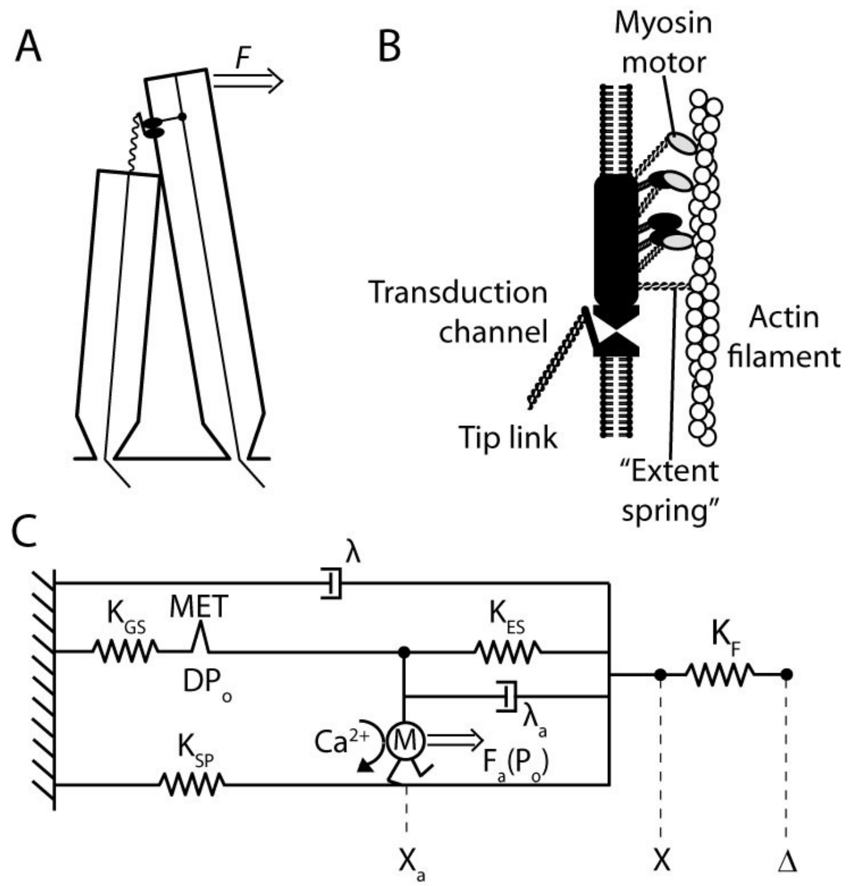

ν, ρ, m, BM-stiffness $\longrightarrow$ μ

A.K. PhD thesis ETHZ 2003

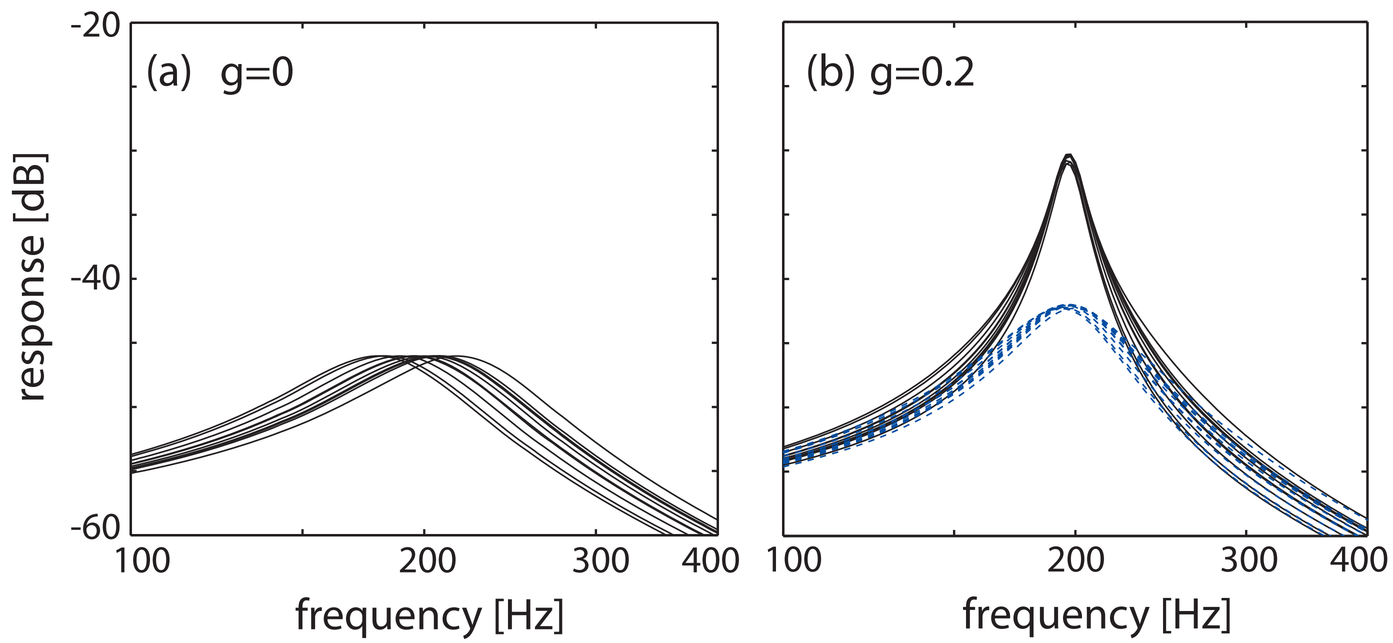

F.G, T.L. & R.S. PRL 2016

no coupling

signal-coupling: signal sharpening !

IV Active elements - fluid coupling:
Computational simplification

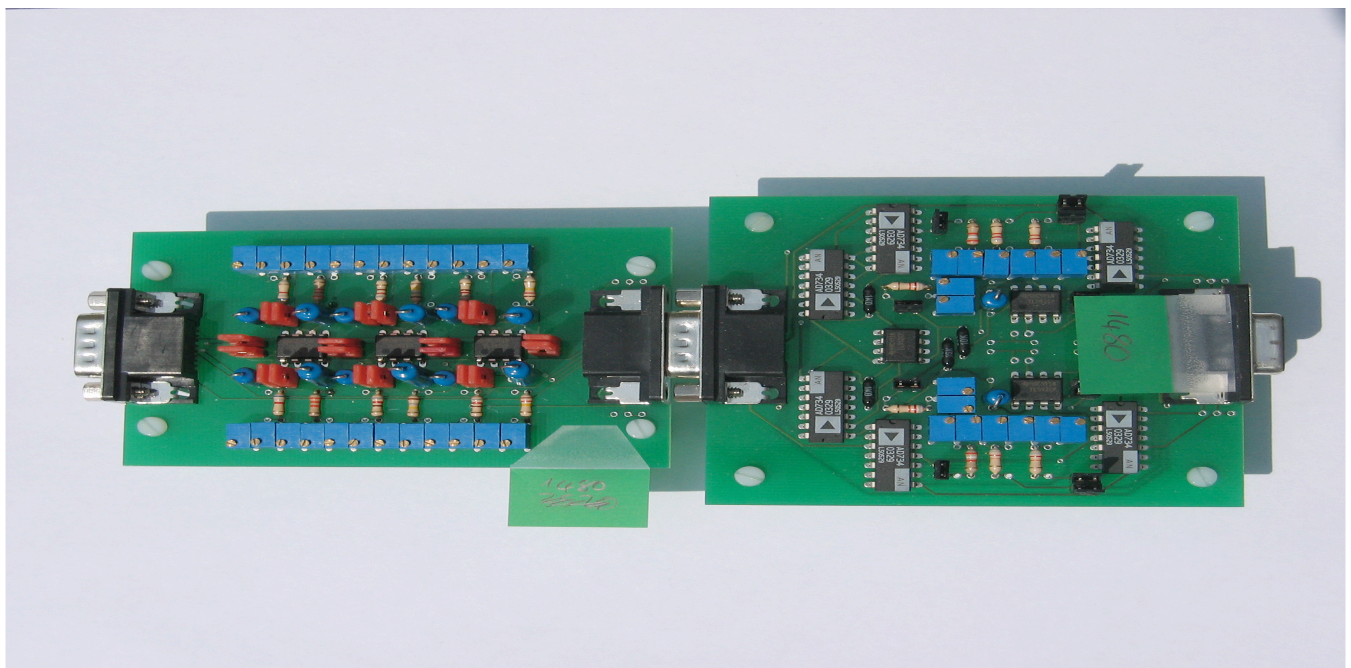

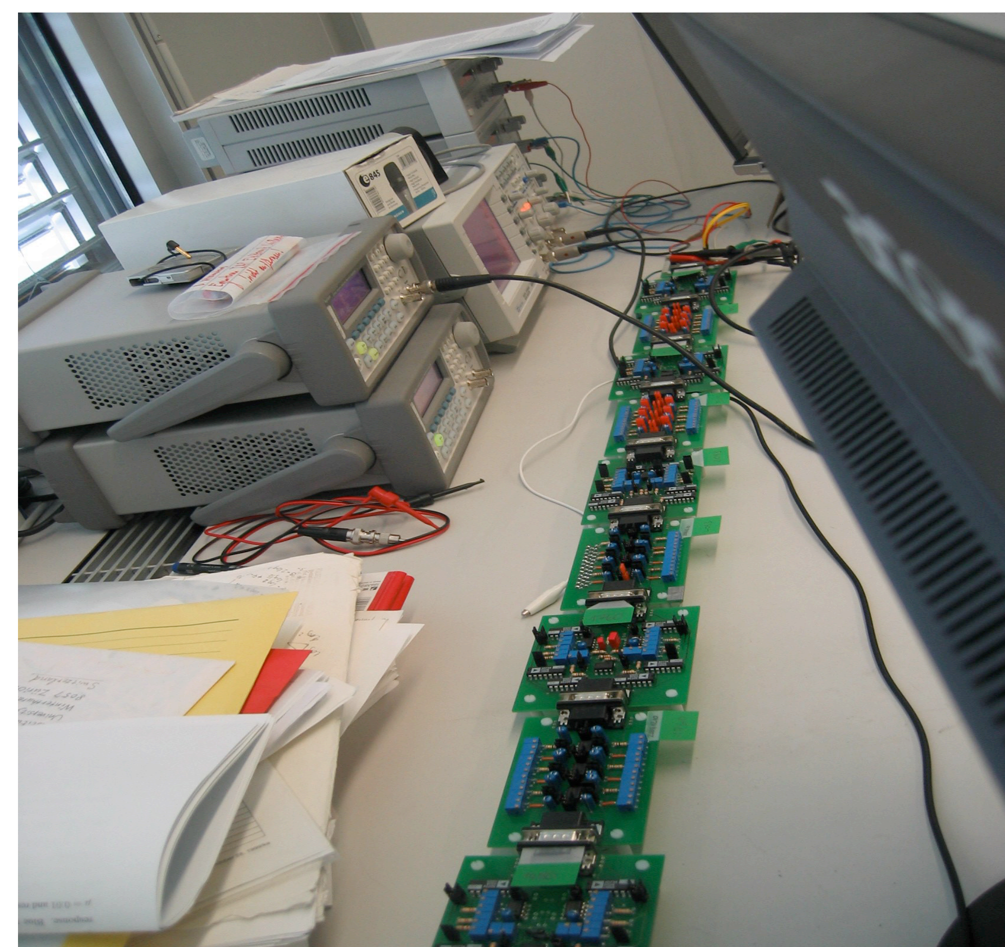

Vyver, Martignoli., R. S. Appl. Phys. Lett. 2008;

US-Patent 2007-2012

‘Hopf cochlea’

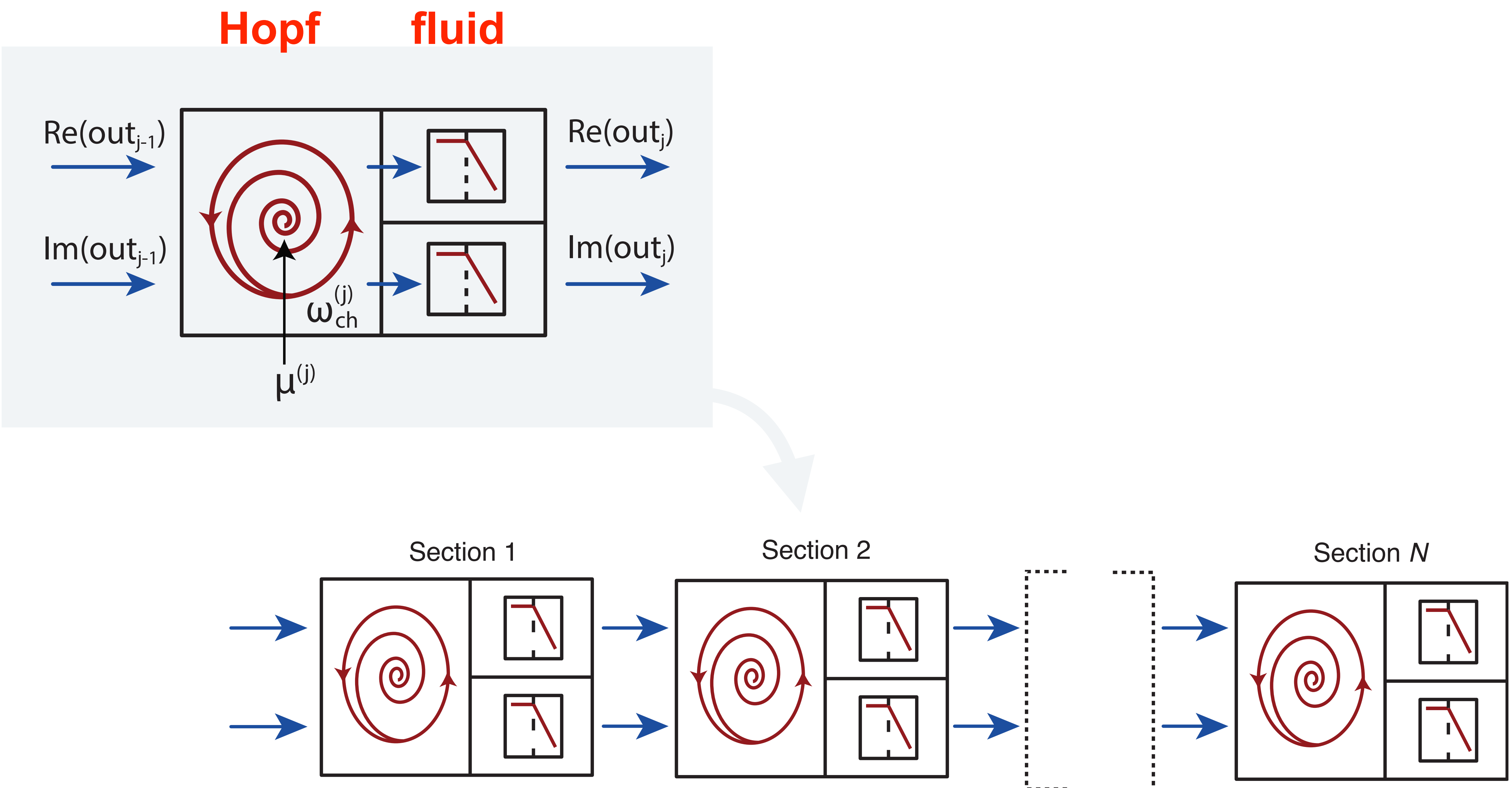

Martignoli, van der Vyver et al. *Appl Phys Lett*, 2007
Martignoli and Stoop *Phys Rev Lett*, 2010
Gomez and Stoop *Nat Phys*, 2014
Stoop and Gomez *Phys Rev Lett*, 2016

Nonlinear phenomena explained:

Mutual suppression by two neighboring tones

experiment

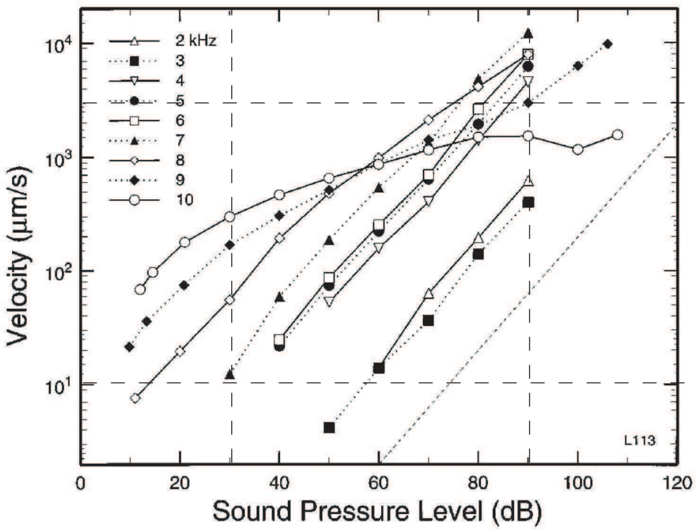

model

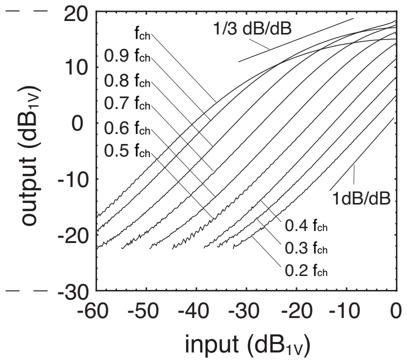

Combination tones

experiment

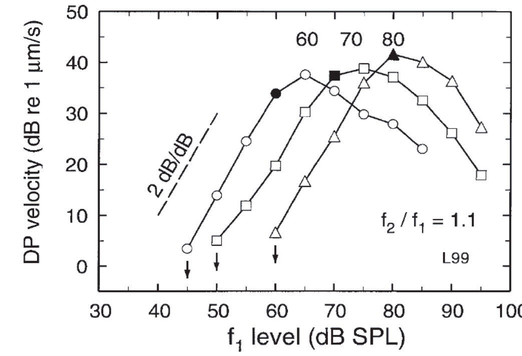

model

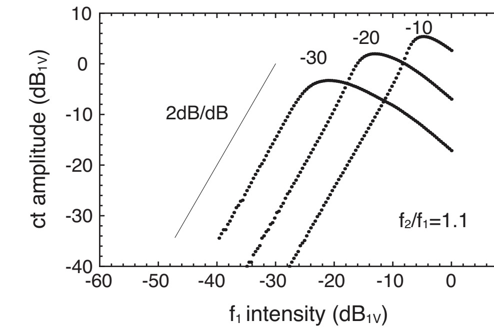

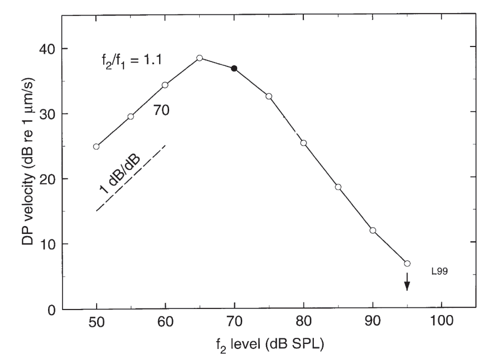

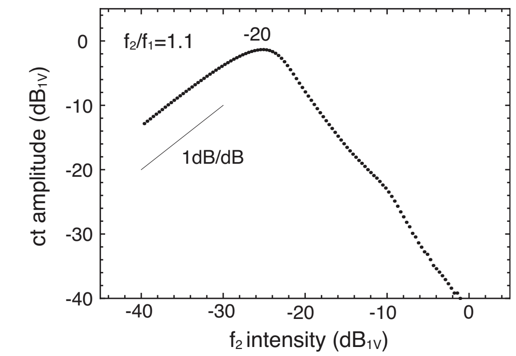

Phase propagation along cochlea

experiment

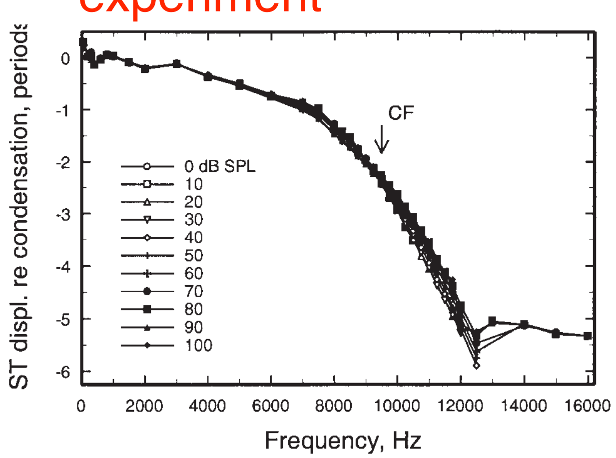

model

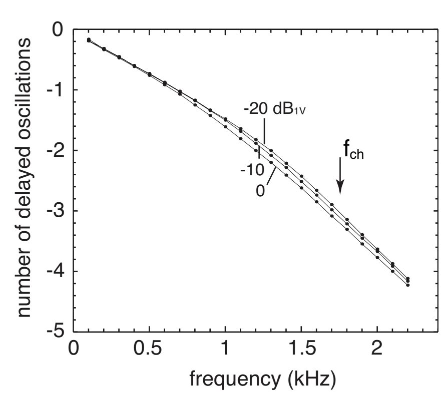

.. and many more, e.g.

Medial olivocochlear efferent stimulation properties

mostly: Stoop and Kern *Phys Rev Lett*, 2004

V Nonlinearity magic

simple signals: complex networks!

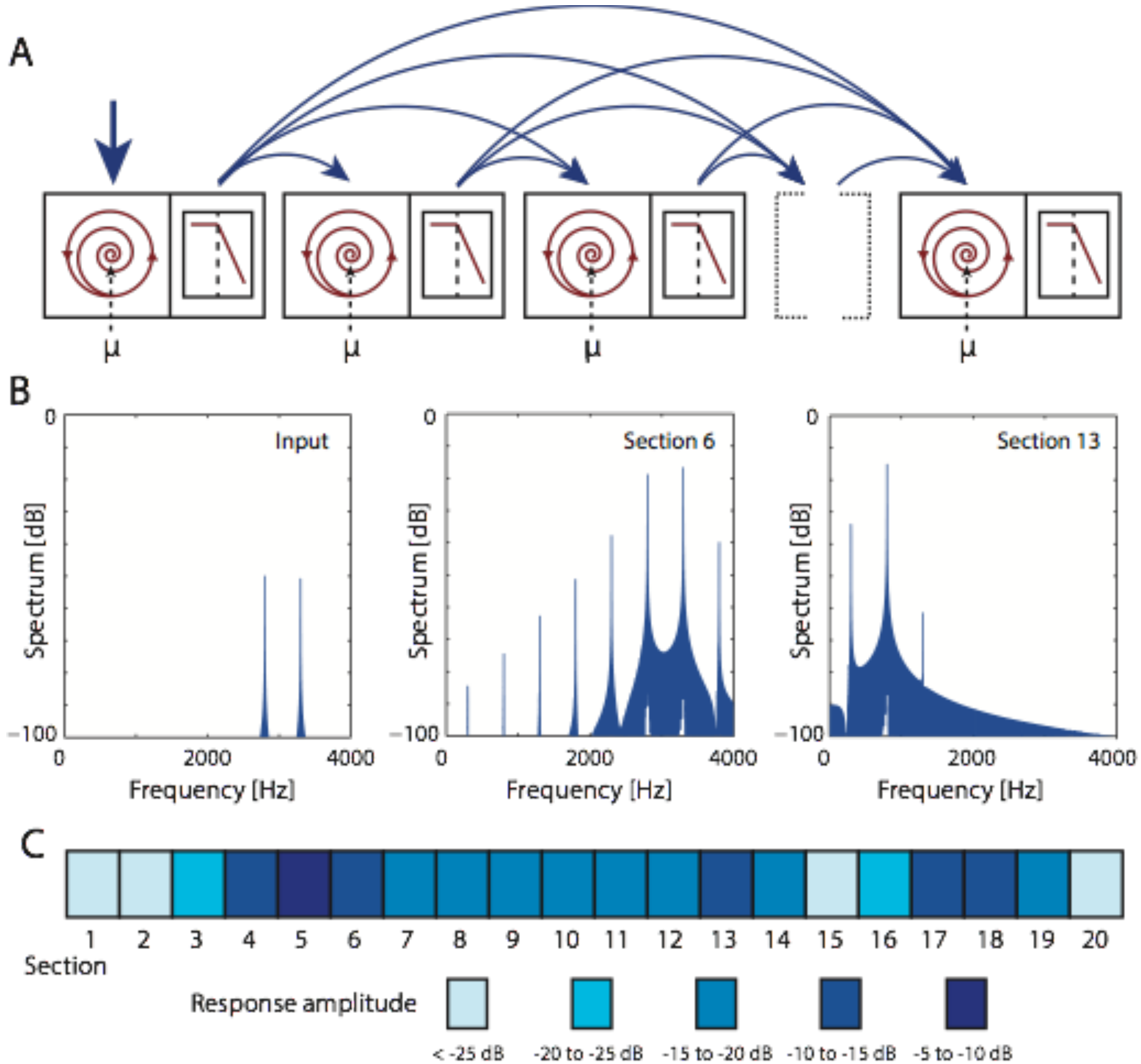

AM sound (f_{car} = 850, f_{mod} = 200 Hz)

inharmonic am tone f(t), A = 0.1, f_{car} = 1.65 kHz,
f_{mod} = 0.2 kHz; waveforms f(t), V(t), Fourier transforms

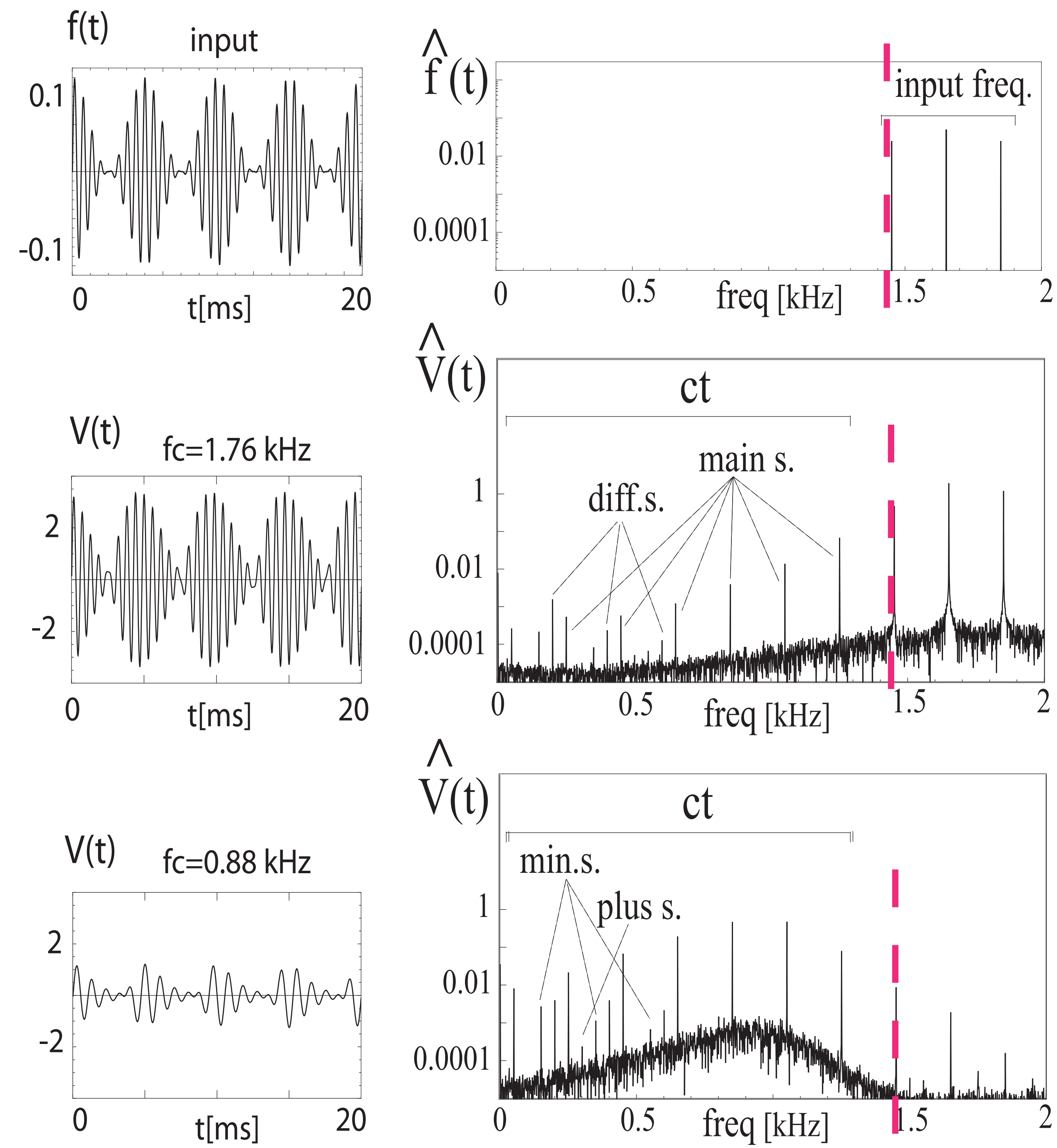

strong ct-generated signal at f_c = 0.88 kHz
that classically should be absent!

(pitch is physical: S.M. & R.S. PRL 2010)

Combination tone saliency:

F.G. & R.S.,, Nat. Phys. 2014

Cochlear excitation for a complex two-tone stimulation (simulated) :

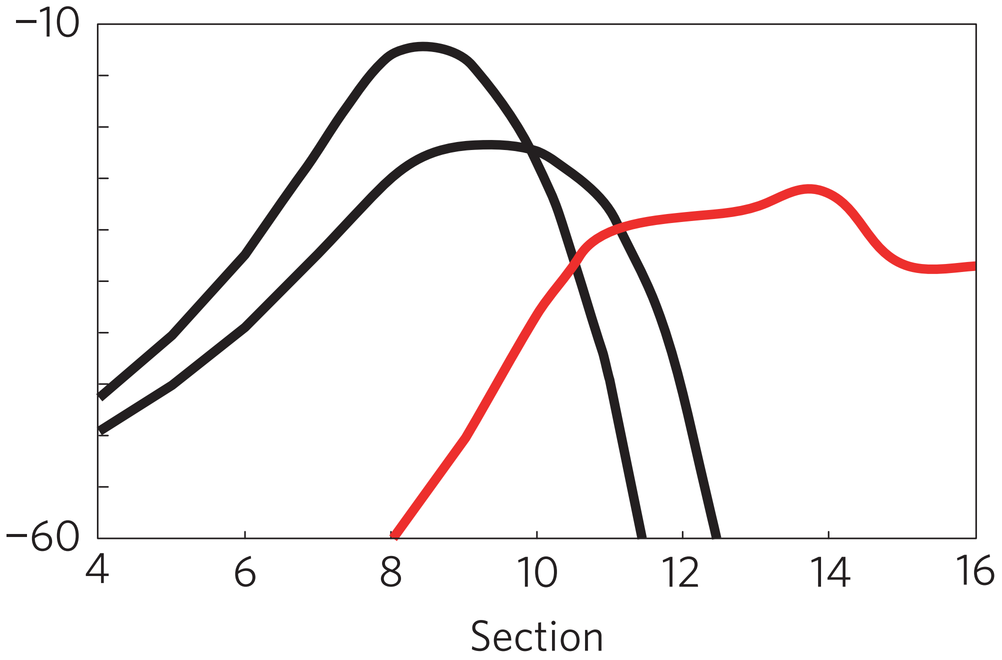

Black: signal power of frequencies f_2 and of f_1
Red: sum of lower CT ($f < f_1$)

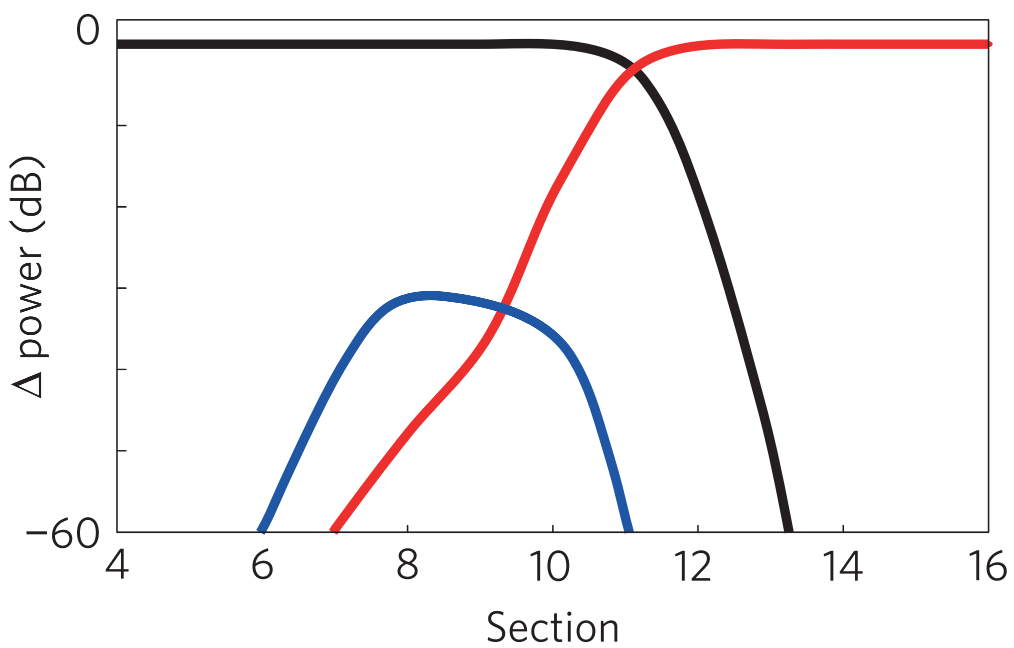

Black: added signal power from frequencies f_1 and f_2
Red: signal power of lower CT
Blue: signal power of higher CT ($f > f_2$) relative to total signal power.

Combination tones:

model

experiment

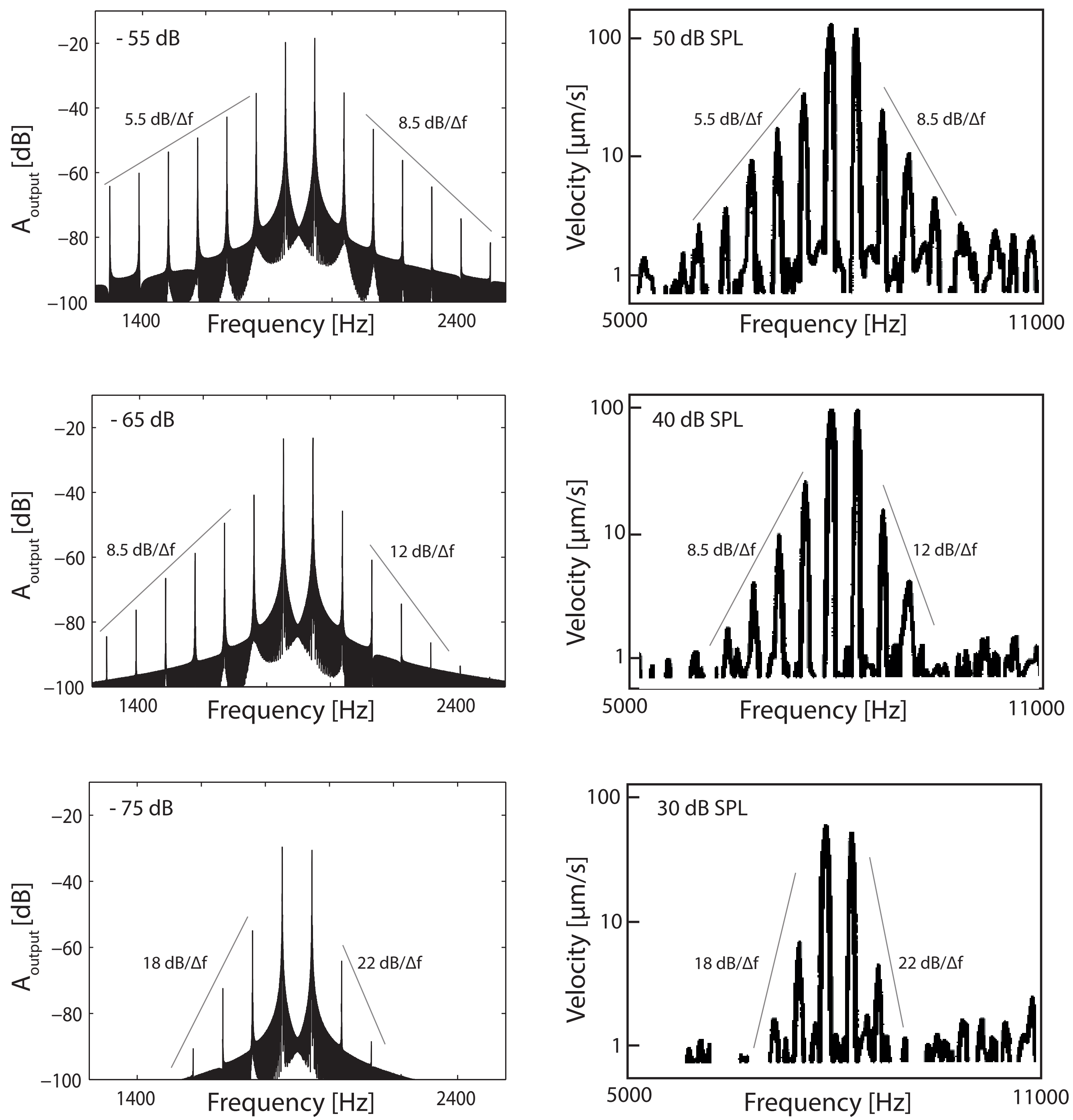

Place of measurement on the tonotopic map and choice of Hopf-cochlea section comparable (roughly one octave from cochlear base).

F.G. & R.S.,, Nat. Phys. 2014

Where is pitch read off ? Smoorenburg:

Perceived pitch = Residual pitch at hearing threshold

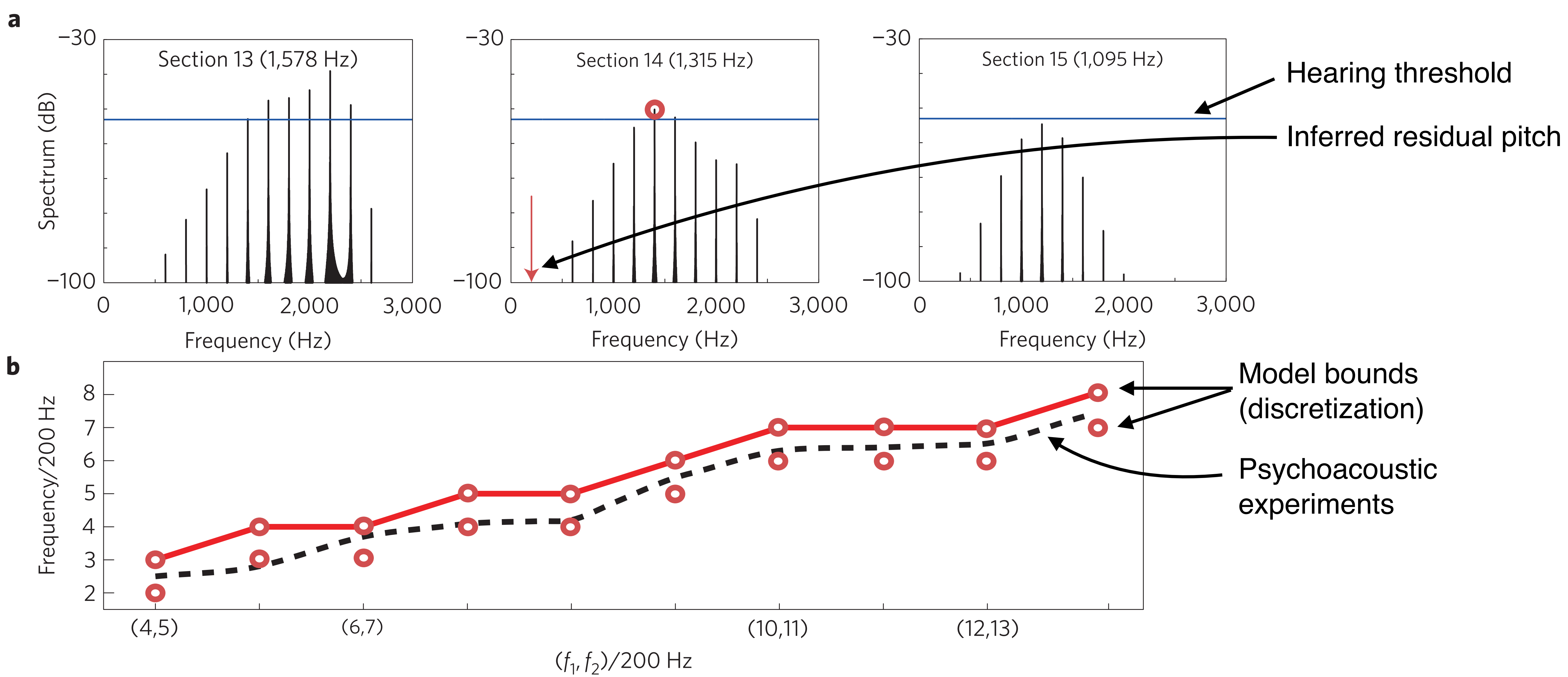

F.G. & R.S., Nat. Phys. 2014

Second pitch shift effect

Two-frequency stimulation f_1 and $f_2 = f_1 + 200$ Hz, cochlea output at $f_c = 622$ Hz (second pitch shift effect): psychoacoustic data (crosses), measured data (full dots)

Inset: ISI-histogram for $f_1 = 900$ Hz, showing fp for k = 4 (left peak, for the rightmost cross) and for k = 5 (right peak, cross at $f_p < 178$ Hz)

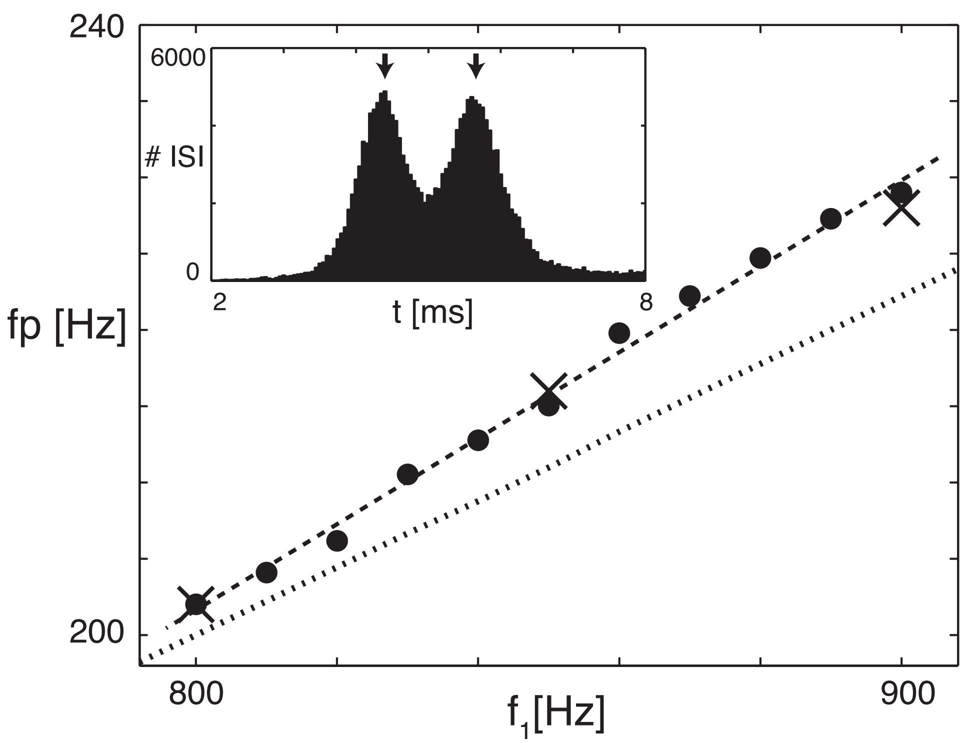

second pitch shift

first pitch shift law $f_p = (f1 + f2)/(2k + 1)$, k = 4, coherently violated

Inset: ISI-histogram end of auditory nerve (S.M., F.G. & R.S. Sci. Rep. 2015)

Second pitch shift:

red: psychophysical experiments; black: model

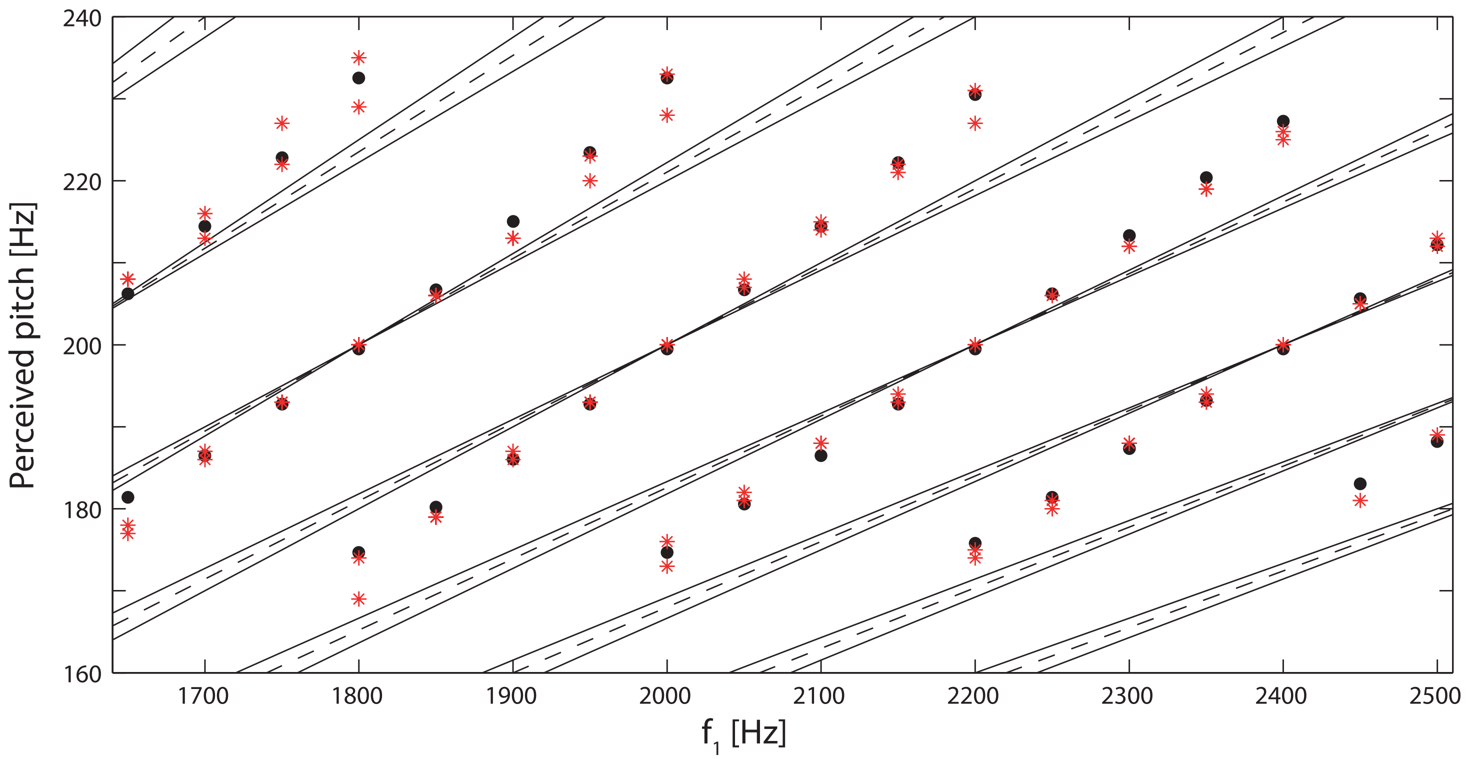

Two-frequency stimuli with $f_2 = f_1 + 200$ Hz.

Red: Psychoacoustic data (partial amplitudes 40 dB SPL)
Black: Hopf cochlea simulation (7th section with f_{ch} = 1245 Hz, partial amplitudes -63 dB).
Solid lines: classical predictions of the perceived pitch.

: solves Ohm-Seebeck dispute !

second pitch shift due to cochlear fluid: F.G. & R.S. Nat. Phys. 2014,
requested slight 'tuning' of the Hopf amplifiers (no-flat tuning of Hopf parameters)

Anatomical embedding

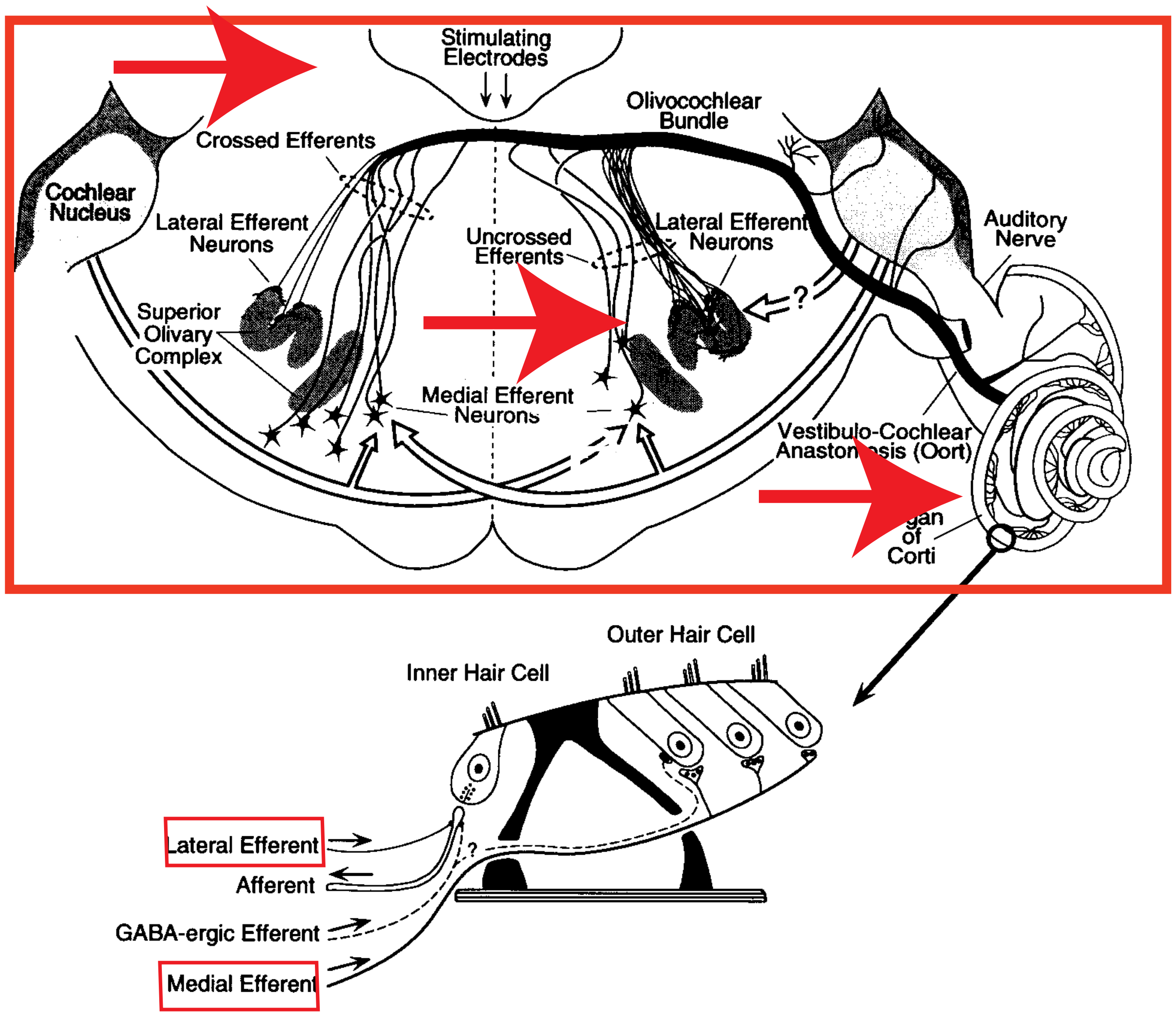

brain

cn (MOC)

cochlea

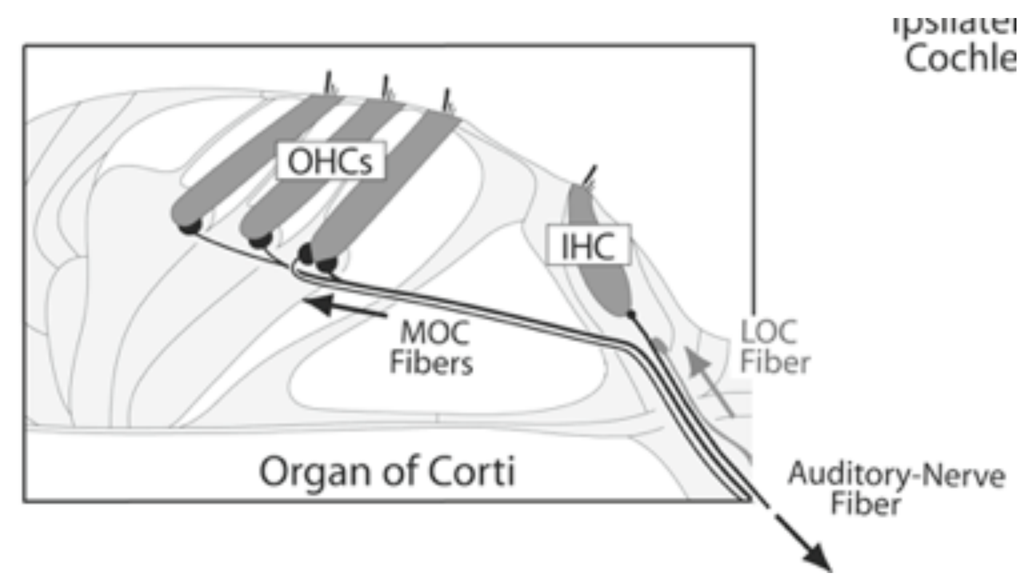

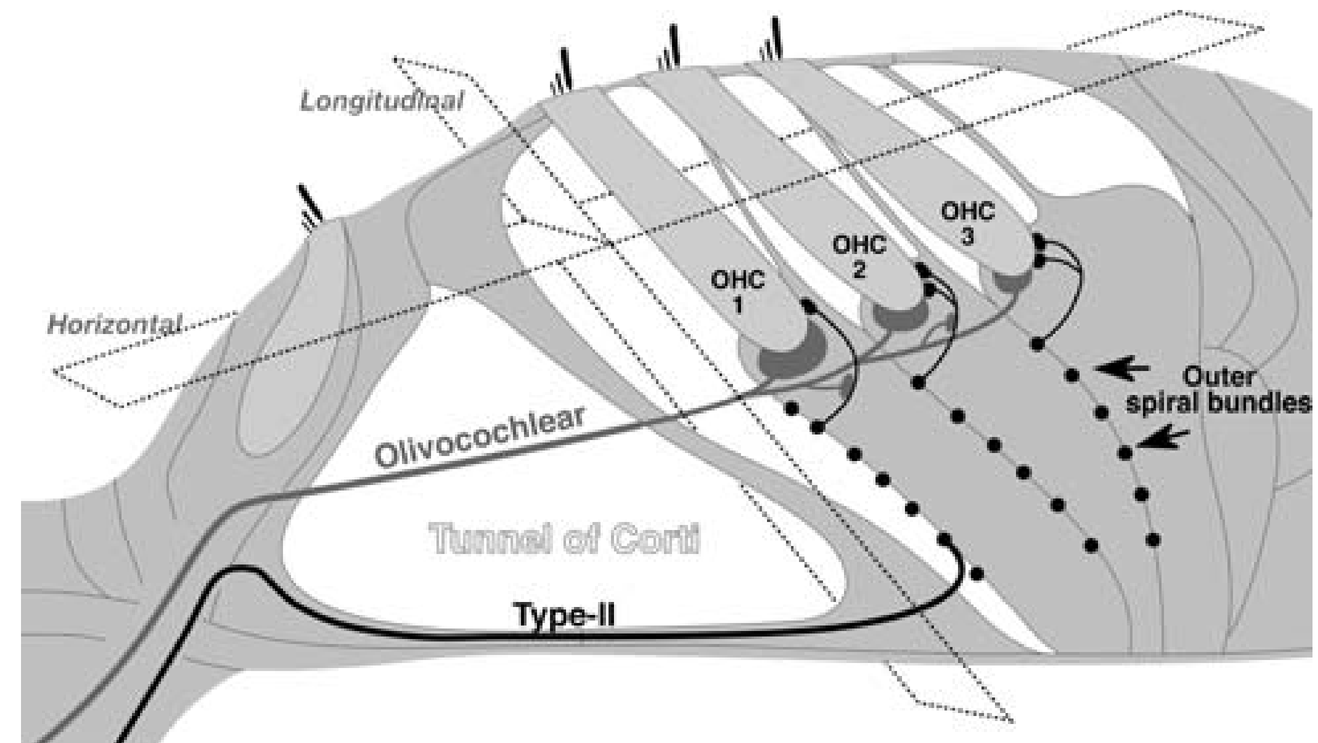

VI Hearing threshold

Animal evidence (nonspecialists)

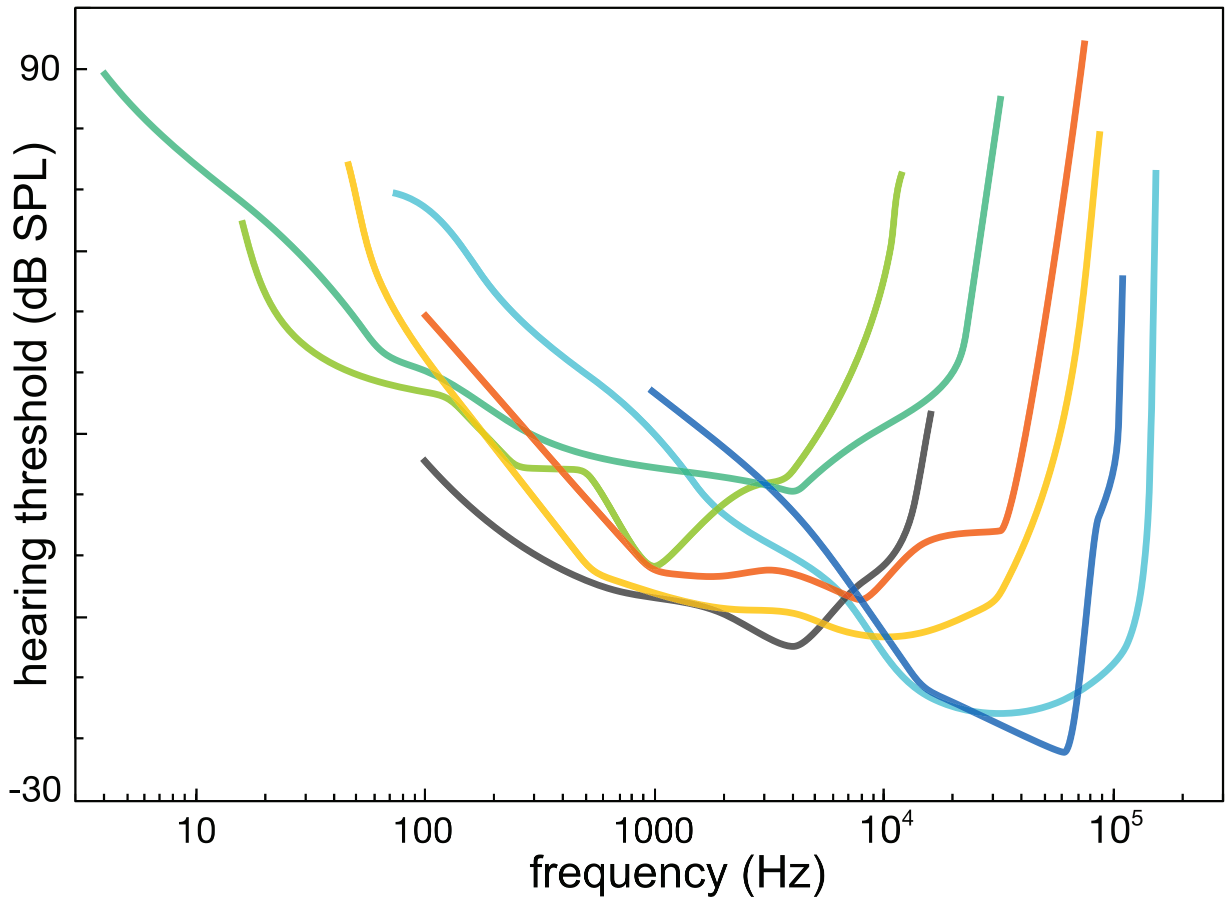

Dogma : Frequency dependence of the hearing threshold is exclusively determined by outer and middle ear

Behavioral audiograms (from top to bottom):

Prairie dog [23], elephant [24], lemur [25], domestic cat [26], human psychoacoustial hearing threshold [4], white-beaked dolphin [27], false killer whale [28].

Animal evidence

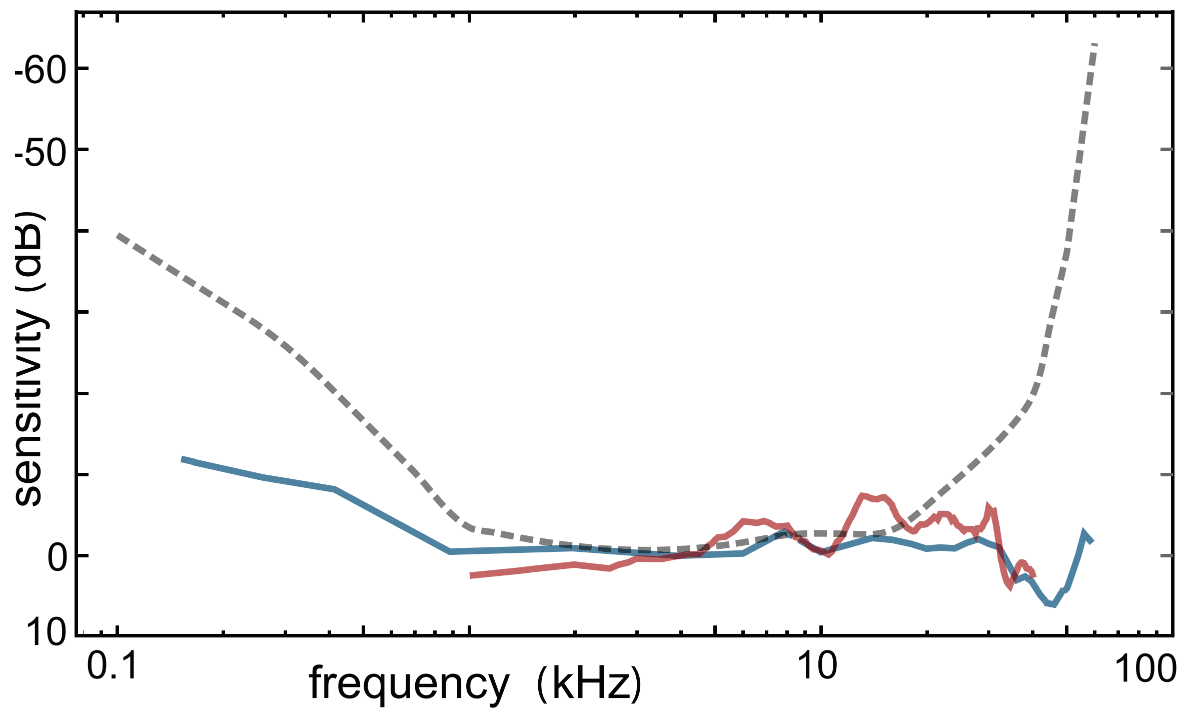

Ruggero and Temchin 2002

Outer-middle ear transfer functions Mongolian gerbil

Dashed: Behavioral hearing threshold
Blue: Pressure in scala vestibuli near stapes footplate
Red: Stapes velocity

Could it be the cochlea?
flat-tuned cochlea:

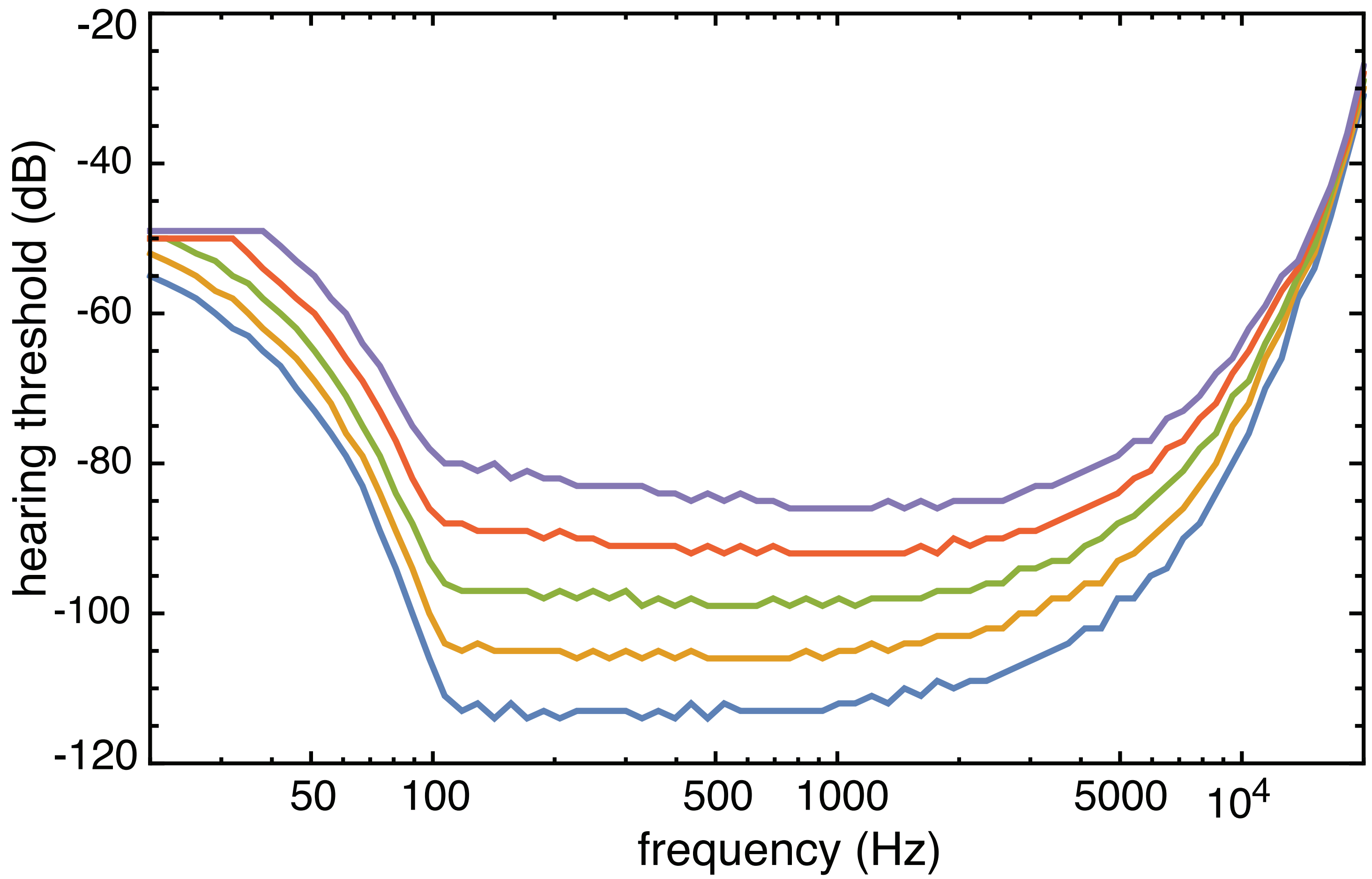

flat tunings: $\mu^{(j)}$ = constant

Hopf cochlea with N=29 sections
f_{ch} = 110…14080 Hz
$\mu^{(j)}$ is the same for all sections:
$\mu^{(j)} = -0.40$
$\mu^{(j)} = -0.35$
$\mu^{(j)} = -0.30$
$\mu^{(j)} = -0.25$
$\mu^{(j)} = -0.20$

F.G., K.K., T.L. & R.S. submitted

1. Response of section j is defined as $R_j = 20\log_{10}[(\max(\mathrm{Re}(out_j))]$
2. The maximal response of Hopf cochlea is $R_{max} = \max(\{R_j : j = 1,2,\ldots,N\})$
3. *Hearing threshold* of a pure tone stimulus $F(t) = A\exp(-i2\pi f t)$: defined as the input level $L = 20\log_{10}[A]$ that gives rise to $R_{max} \simeq -50$ dB
4. 0 dB SPL input in experiments corresponds to -114 dB input to Hopf cochlea

Tuning of amplifiers

$\mu^{(j)}$ detuning as in Smoorenburg

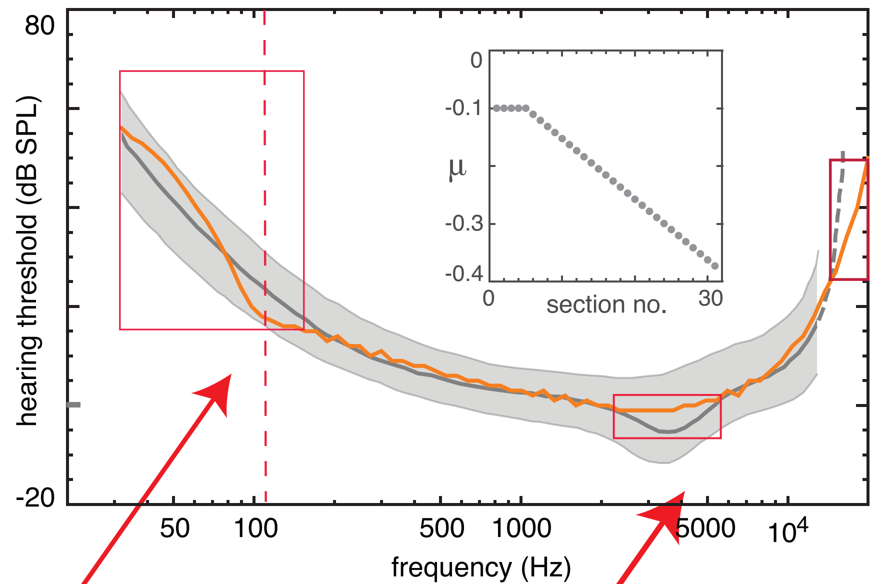

no data available

gray: human variability (Fastl / Zwicker 2007)

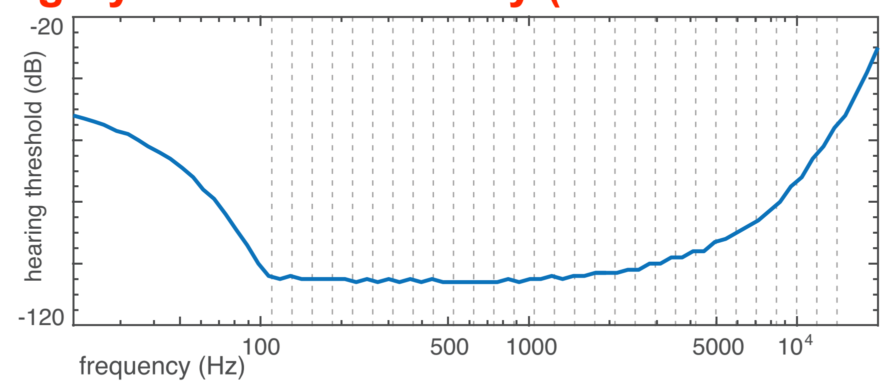

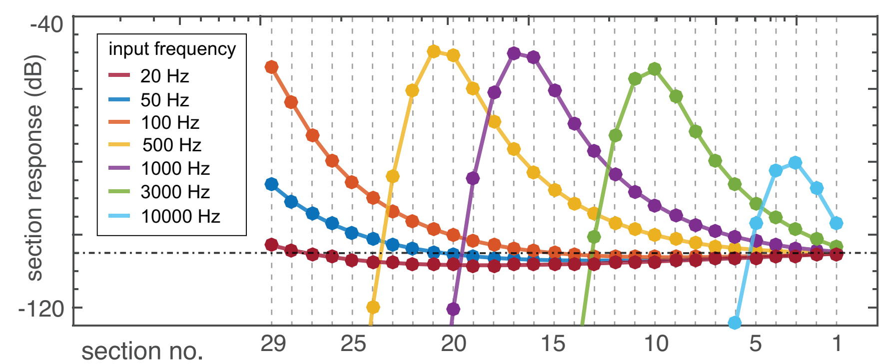

discretization effect

resonance middle/outer ear: <10 dB, around 4000 Hz (Shaw 1974): Perfect agreement

contradiction to schoolbook wisdom ..

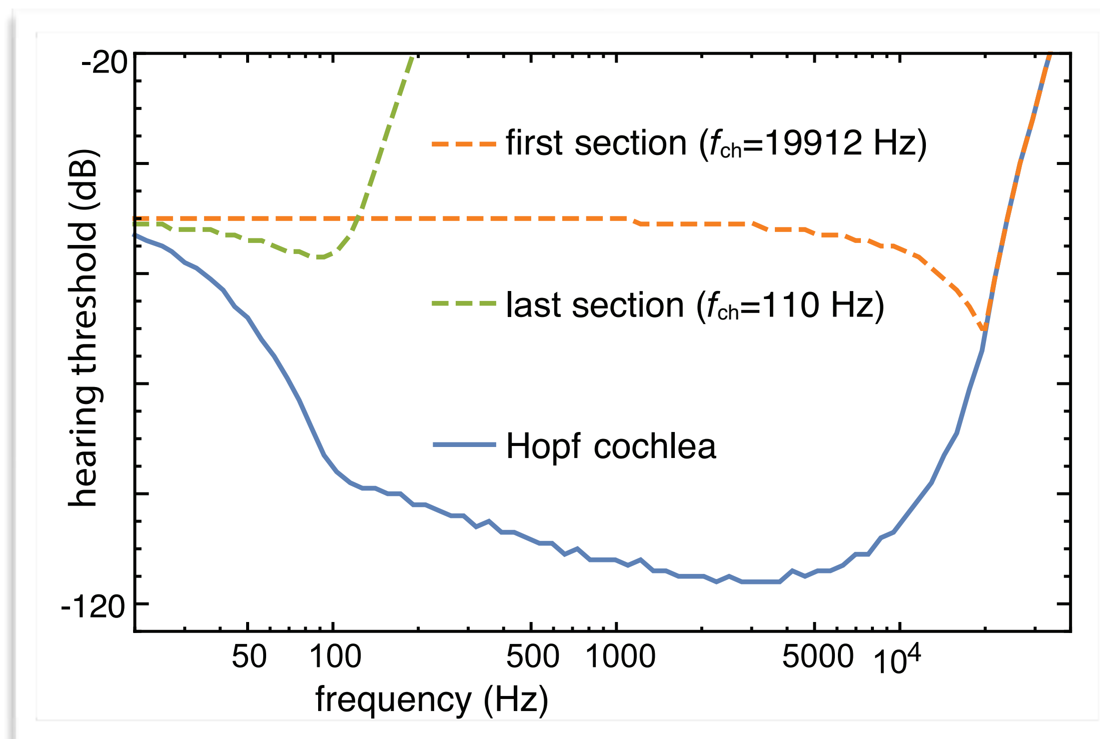

VII Activation networks are the signal..

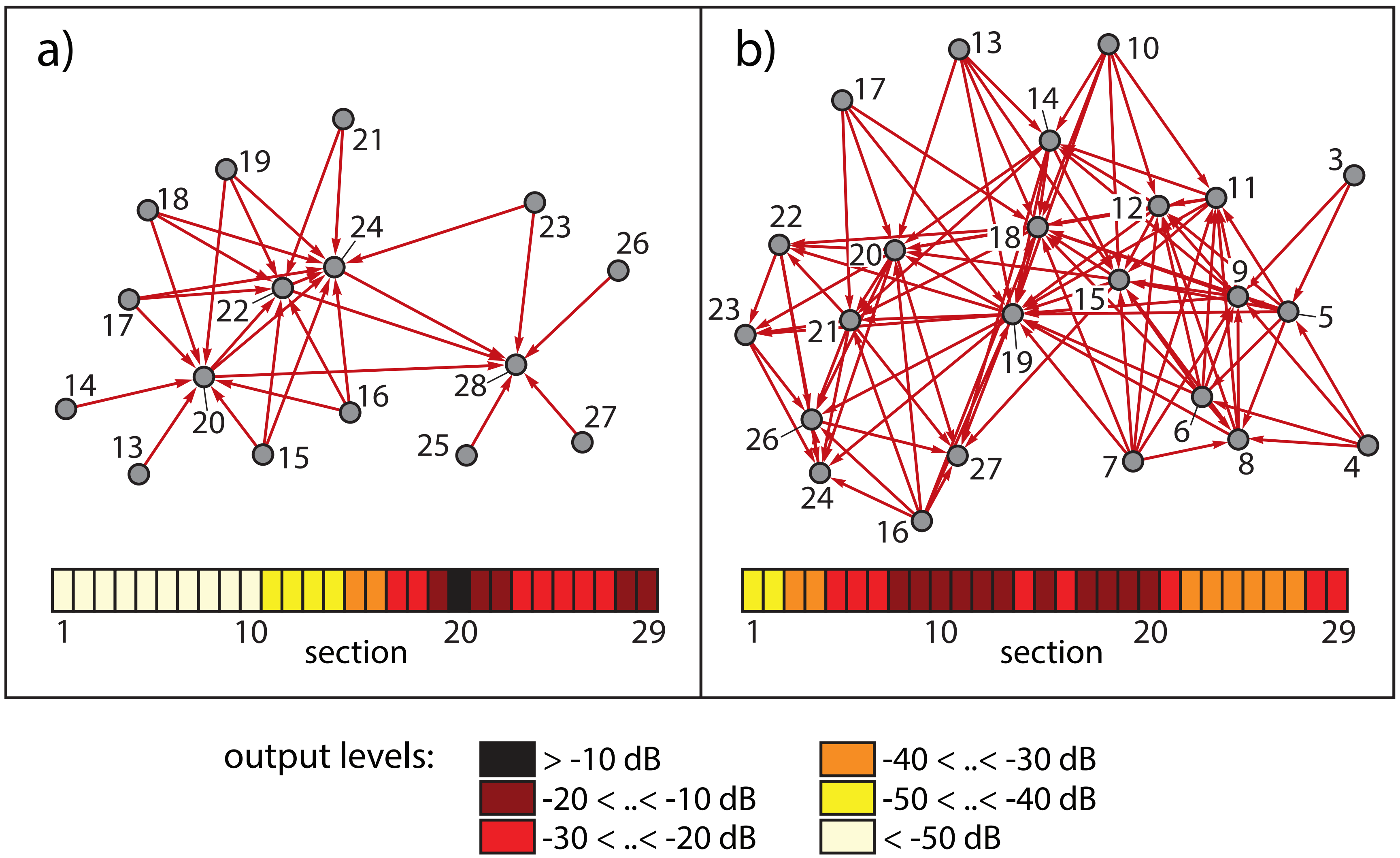

a) two pure tones input (3/8, 1/2 kHz)

b) two complex tones (2, 3.35 kHz, with 5 harmonics each)

Cochlea: 29 sections, covering (0.11, 14.08) kHz on a logarithmical scale; μ=-0.25 at all sections; input: -60 dB each tone. Upper: Activated networks (='above hearing threshold'), lower: corresponding activations on the unrolled cochlea.

(R.S. & F.G. PRL 2016)

VIII Hearing @ criticality?

Two complex tones (random amplitude and frequency):

s: size of activation network by number of links

Inset: fixed amplitudes:
subcritical, critical, supercritical

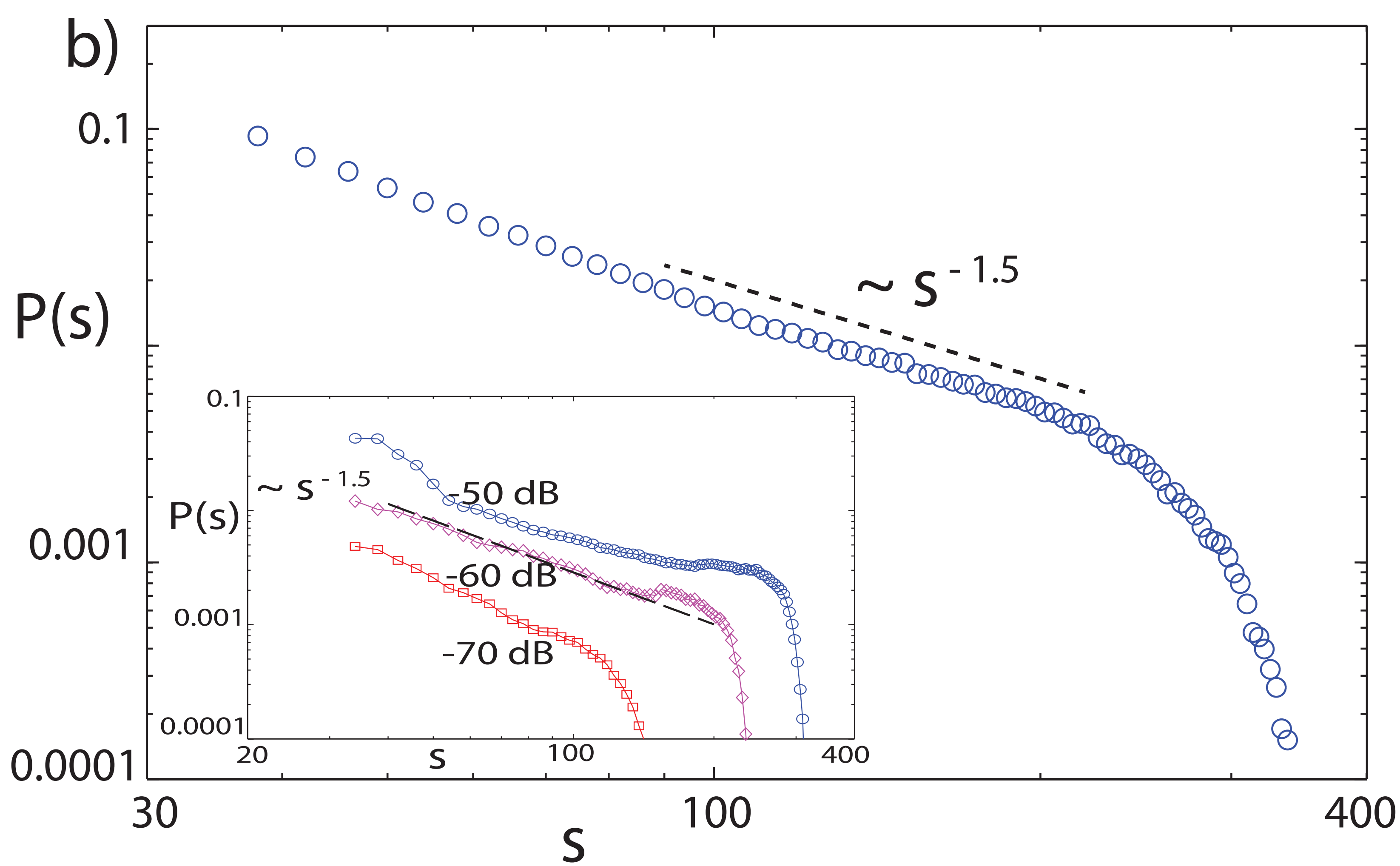

power-law activation networks!

(R.S. & F.G. PRL 2016)

Statistical meaning of learning

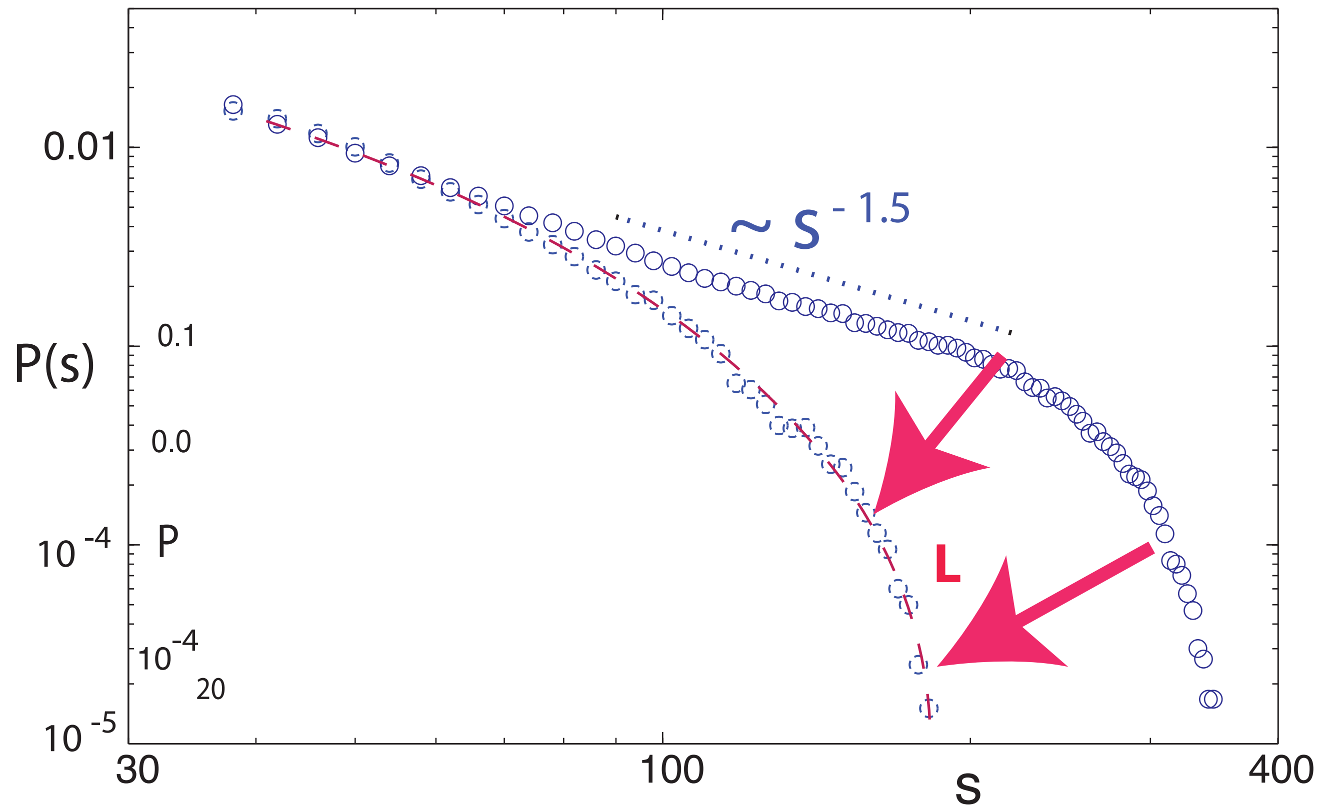

Detuning of two frequency bands (nodes 15,16 and nodes 19,20,21) from $\mu = -0.25$ to $\mu = -2.0$: The initial power-law distribution $s^{-1.5}$ changes into a strictly convex distribution shape (line L)!

IX When is a sound perceived harmonic?

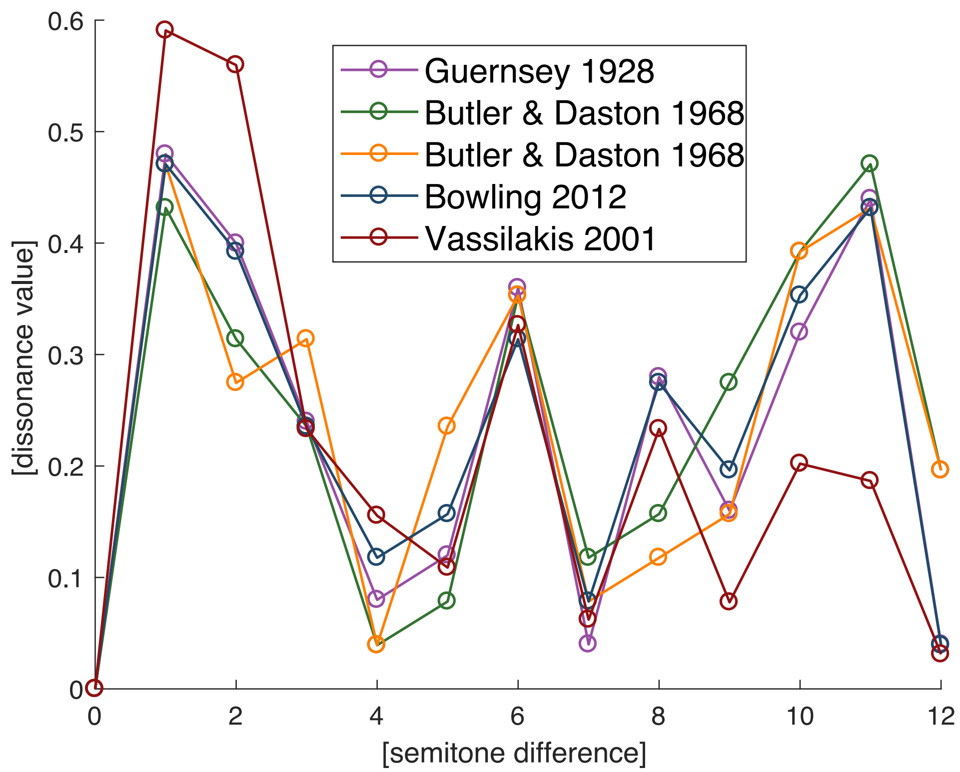

Dissonance vs. interval length:
Not cultural, but strong experimental variations

Short history of consonance and dissonance:

Pythagoras (6^{th} century BC):
Strings of simple length ratios elicit sensations of pleasantness ("consonance").
Intervals of the octave (2:1), the perfect fifth (3:2) and the perfect fourth (4:3) provide the Pythagorean tuning.

Geoseffo Zarlino (renaissance music theorist):
Added the intervals of the major third (5:4), minor third (6:5) and major sixth (5:3) to the consonance set.

Daniel Bernoulli: Superposition of infinite harmonic vibrations on a vibrating string;
Marin Mersenne, Leonhard Euler and Joseph Fourier: Concept of a "harmonic series".

Professionals vs. amateurs: Identically perceived

Pure tones vs, complex tones: Distinctly perceived

Network property?

Network picture

Higher dissonance <—>

larger activated network size,

larger edge density

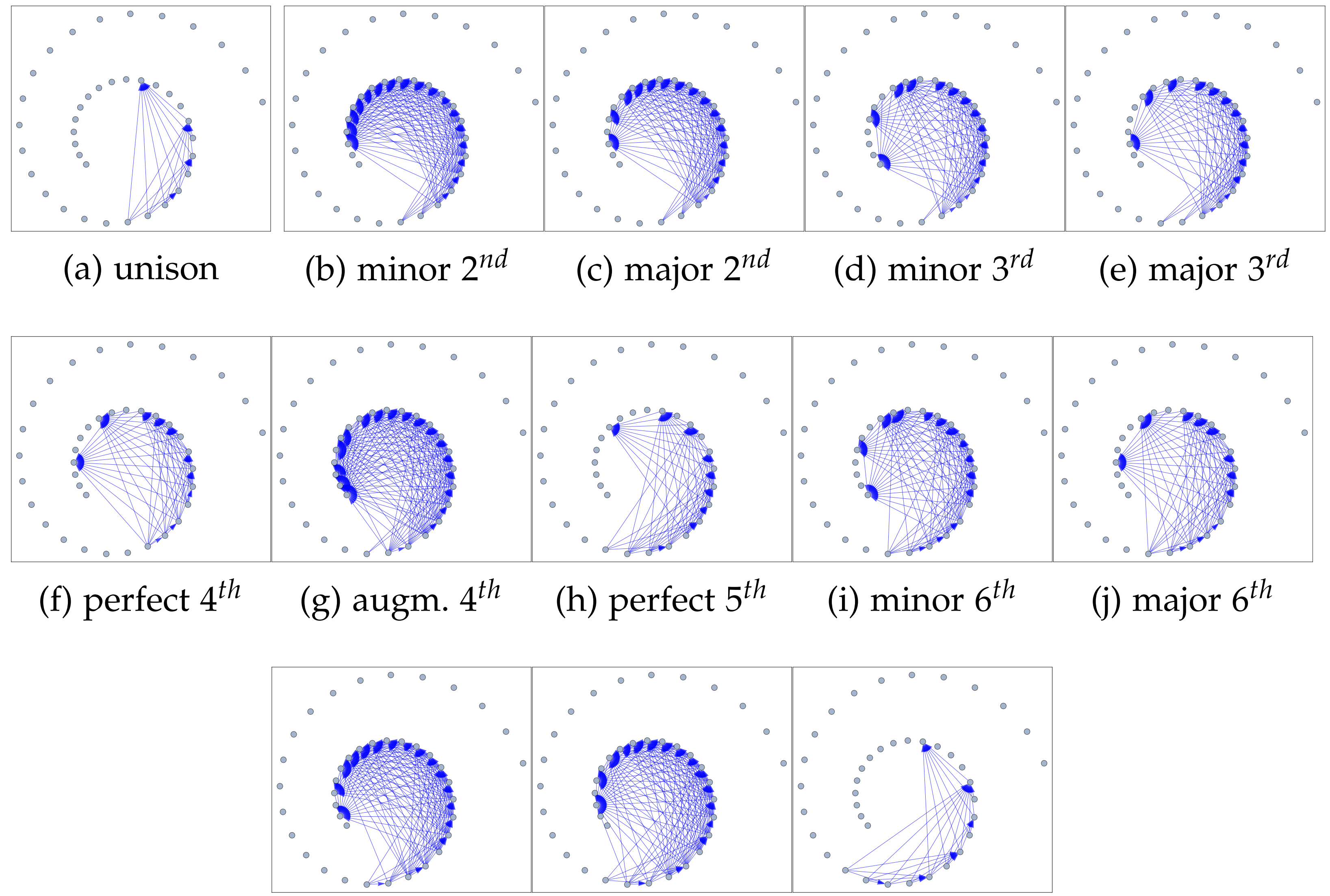

(a) unison (b) minor 2^{nd} (c) major 2^{nd} (d) minor 3^{rd} (e) major 3^{rd}

(f) perfect 4^{th} (g) augm. 4^{th} (h) perfect 5^{th} (i) minor 6^{th} (j) major 6^{th}

(k) minor 7^{th} (l) major 7^{th} (m) perfect 8^{th}

Network-based measures of dissonance:

.

- Topological graph: Network size of active nodes (SLM)
- Weighted graph (WLM)

Network measure vs. psychoacoustics:

experiment

model

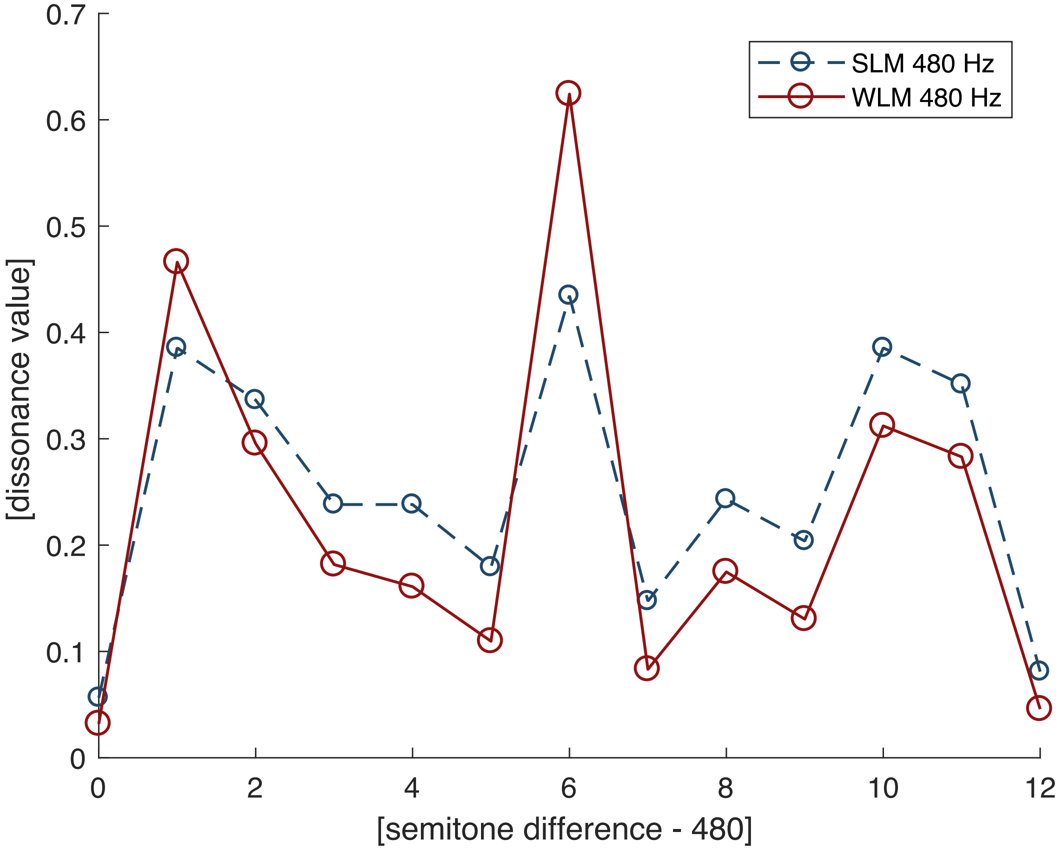

Not perfect, but a good match!

Perspectives of this approach:

- perfect restitution of human hearing
- new generations of technical sound sensors
- dealing efficiently and coping with ‘big data’

Fundamental human perception ‘reduced’ to cochlear physics and network theory

: Physics / engineering approach brings us closer towards the “human mind”

thanks for listening..

Measuring listening efficacy

(F.G, V.S., N.B., R.S., Phys. Rev. Appl. 2014)

models of pitch perception suggest comparison:

- SACF: sum of normalized autocorrelations of each section's output
  vs.
- NACF: normalized autocorrelation of the target signal
  desired signal x / unwanted signal y / f_i output of i-th section

$$\boxed{TE\,(x,y) := \frac{||\mathrm{NACF}(x) - \sum_i \mathrm{NACF}(f_i(x+y))/N||_2}{||\mathrm{NACF}(y) - \sum_i \mathrm{NACF}(f_i(x+y))/N||_2}}$$

TE in [0,infinity]:
high (>>1) TE: bad tuning, low (<1): (very) good tuning

:TE-optimization problem in multidimensional μ-space

Results :

two complex instruments:
'Flute' vs.'Zinke'(both parts of church organs)

Tuning patterns: red: close to bifurcation,
blue: away from bifurcation.
red: close to bifurcation,

a) left: sweeping "Reel" target
right: sweeping "Flute" target
(tuning towards "Reel" requests
enhancement of the 3rd and 5th harmonics
(two parallel reddish stripes)

TE consistently < 1:
strong target enhancement
Black: flat tuning; red: TE-tuning

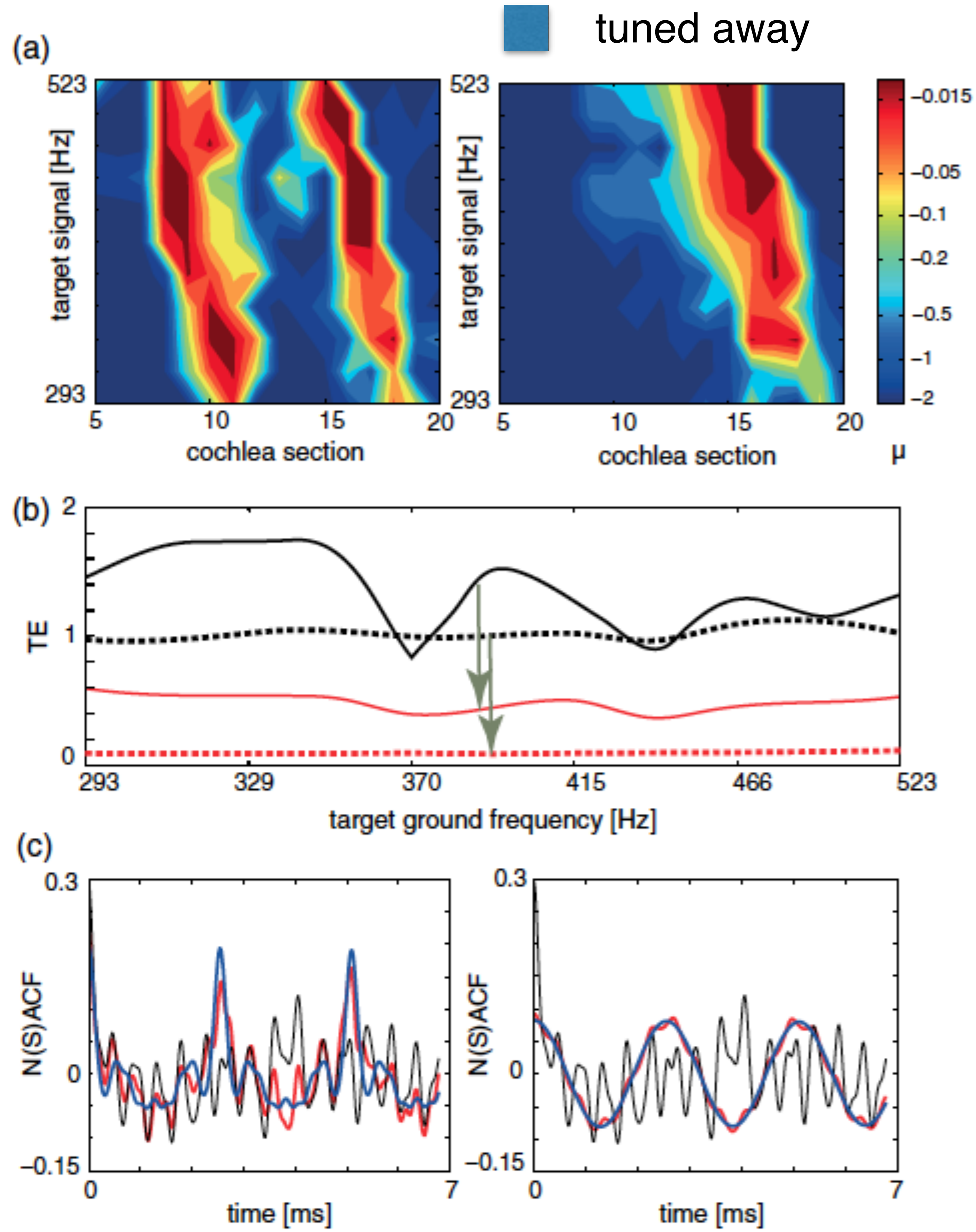

(F.G, V.S., N.B., R.S., Phys. Rev. Appl. 2014)

Using pitch as guiding control feature:

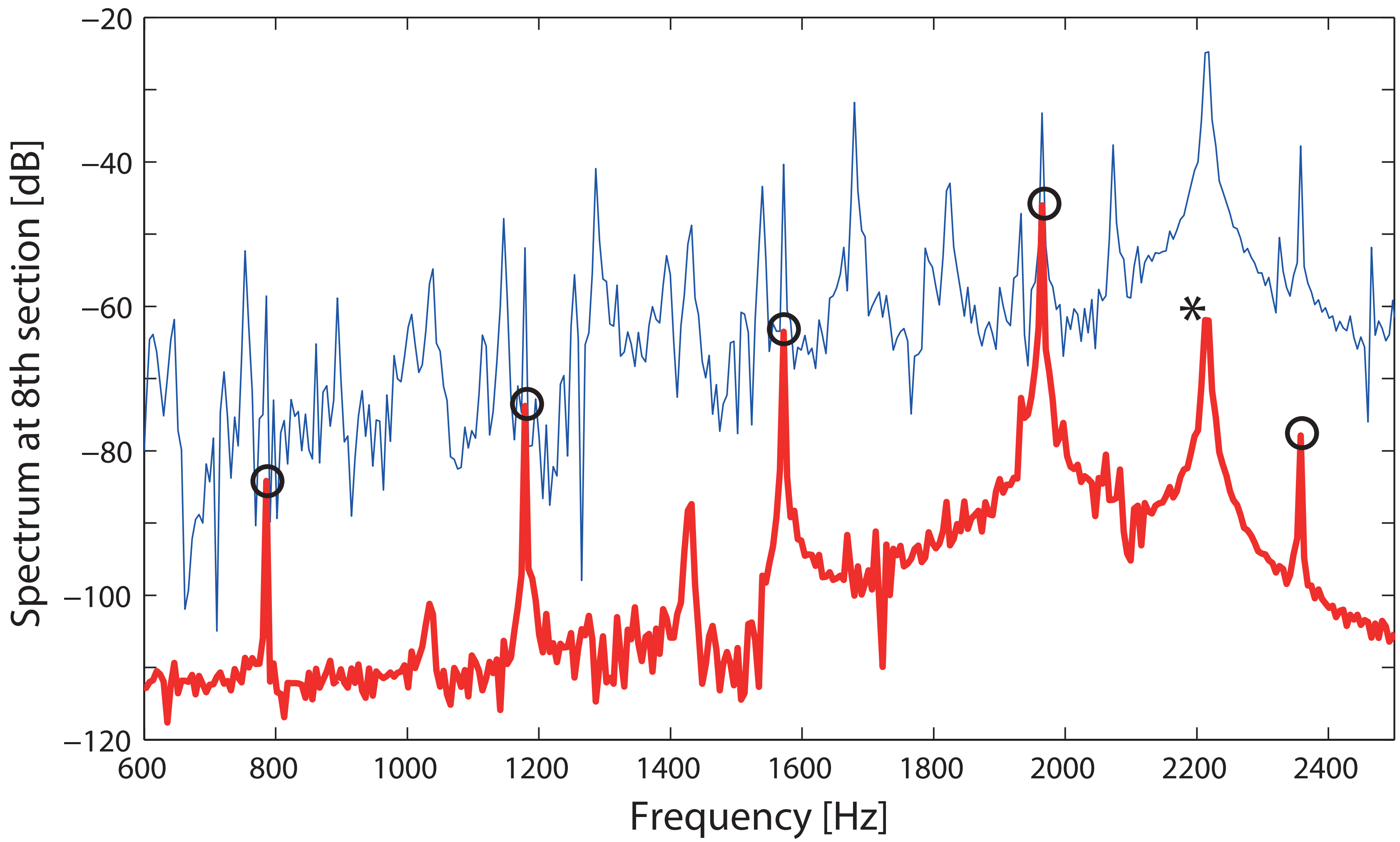

original: flute and reel

disturber (flute) and crossproducts removed; harmonic series restored

: efficient biomorphic tool for source separation!

(F.G.,V.S.,N.B., R.S.. Phys. Rev. Appl. 2014)

Hearing threshold

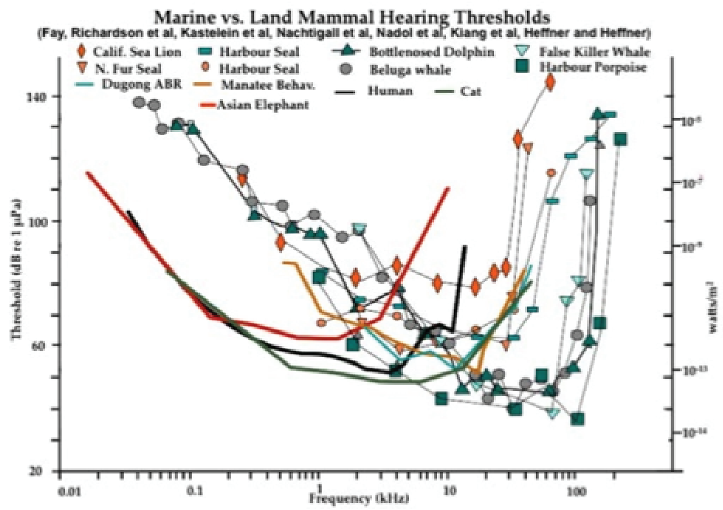

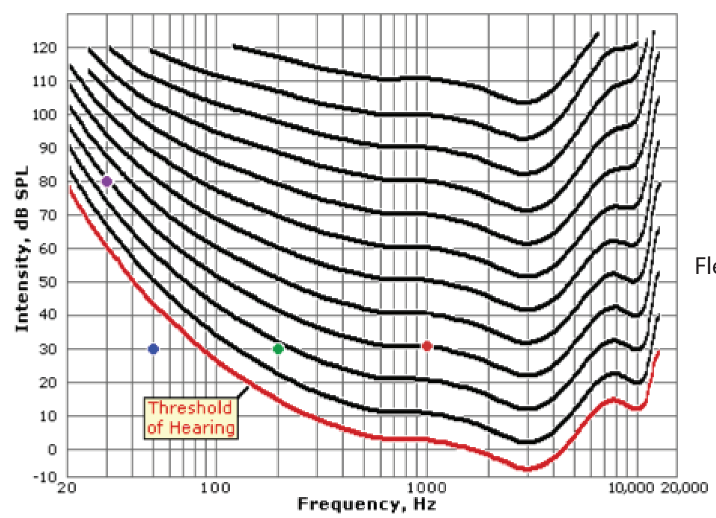

Fletcher-Munson Curves

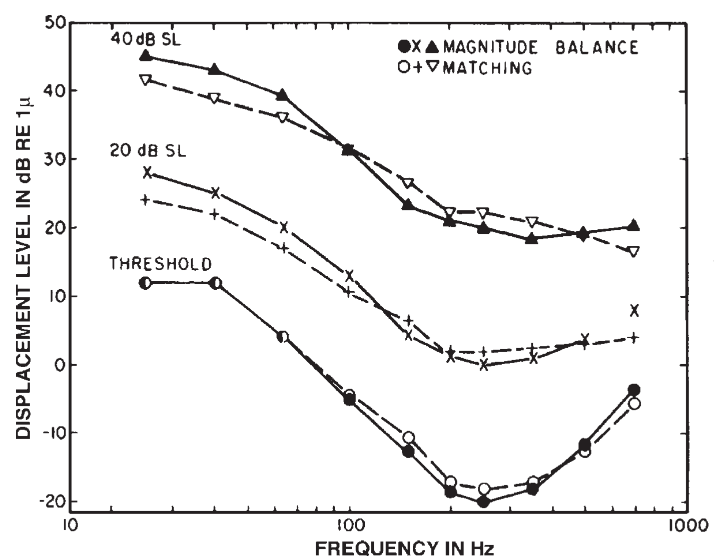

Verrillo et al. (1969)

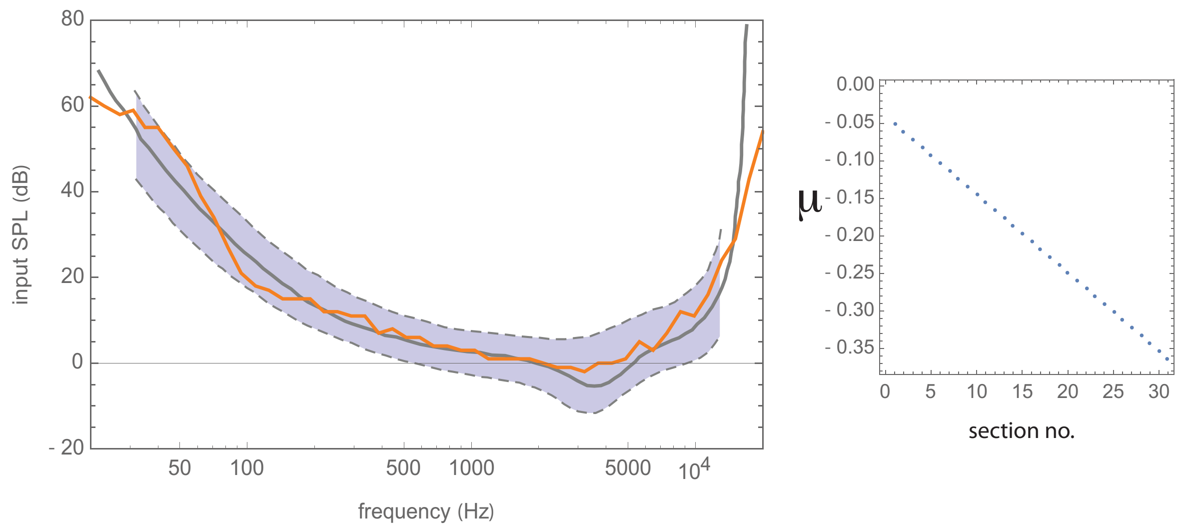

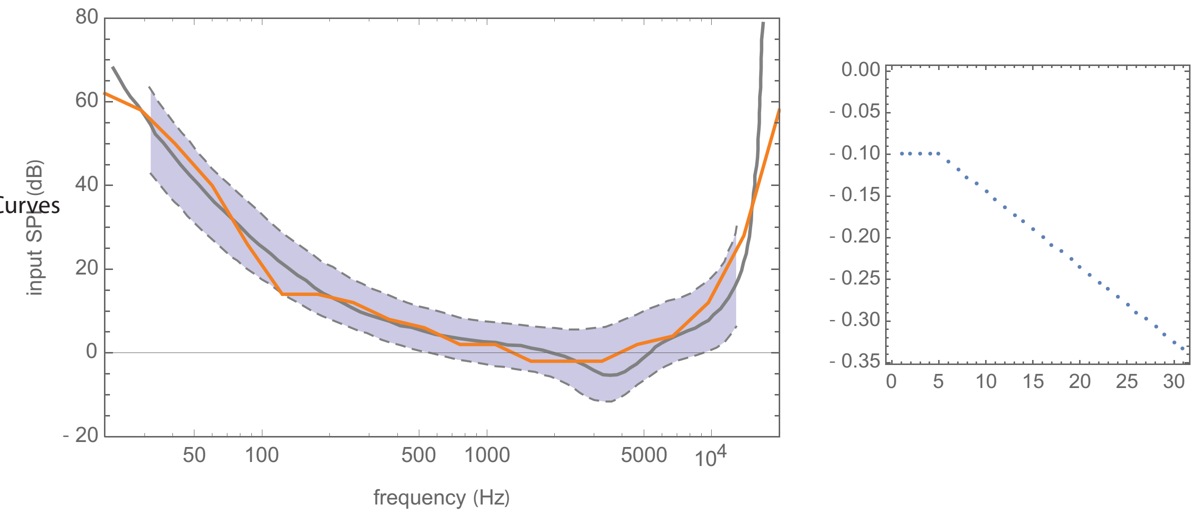

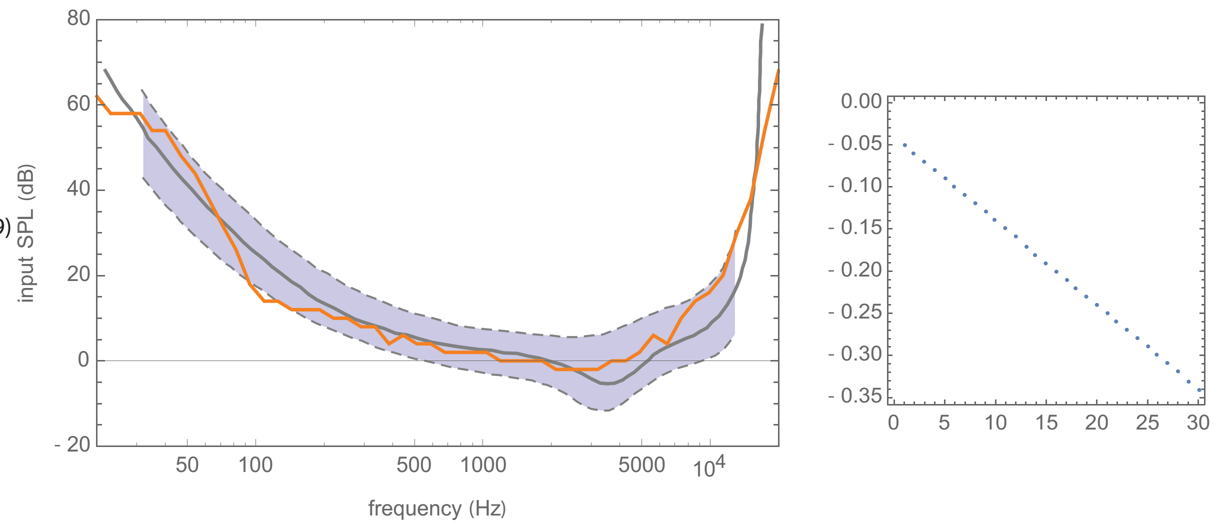

Verrillo, R.T., Fraioli, A., and Smith, R.L. Sensory magnitude of vibrotactile stimuli. Percept. Psychophys. 6: 366–372, 1969..

Measuring listening efficacy

models of pitch perception suggest comparison:

- SACF: sum of normalized autocorrelations of each section's output
  vs.
- NACF: normalized autocorrelation of the target signal
  desired signal x / unwanted signal y / f_i output of i-th section

$$\boxed{TE(x,y) := \frac{||\mathrm{NACF}(x) - \sum_i \mathrm{NACF}(f_i(x+y))/N||_2}{||\mathrm{NACF}(y) - \sum_i \mathrm{NACF}(f_i(x+y))/N||_2}}$$

TE in [0,infinity]:
high (>>1) TE: bad tuning, low (<1): (very) good tuning

:TE-optimization problem in multidimensional μ-space